

supporting information

9,9-Dialkylfluorene-alt-benzothiadiazole based bolaamphiphiles with formation of complex self-assembled liquid-crystalline phases of cubic A15 network and $Col_{sq}/p4gm$ at the triangle-square transition

Shibo Chen,^a Haixia Wu,^b Zilong Guo,^a Qingqing Han,^a Jiaming Liu,^a Yu Yang,^{b*} Xiaohong Cheng^{a*}

^a Key Laboratory of Medicinal Chemistry for Natural Resource, Ministry of Education; Yunnan Research & Development Center for Natural Products; School of Chemical Science and Technology, Yunnan University, Kunming, 650091, P.R. China. E-mail: xhcheng@ynu.edu.cn

^b School of Materials and Energy, Yunnan University, Kunming 650091, P. R. China. E-mail: yuyang@ynu.edu.cn

Content

1. Additional Experimental Data	S2
2. Material synthesis and analytical data	S11
3. References	S34

1. Additional Experimental Data

1.1 Experimental techniques

Polarizing Optical Microscopy (POM): Optical textures of all compounds were characterized by polarizing optical microscopy (Leica DM2700P) with the combination of a heating stage and controller (Linkam T9). Optical investigations were carried out under equilibrium conditions between two glass slides that were used without further treatment. A full wavelength retardation plate was used to determine the sign of birefringence.

DSC measurements: Transition enthalpies were obtained by differential scanning calorimetry (DSC), which was recorded on a DSC 200 F3 Maia calorimeter (NETZSCH) in sealed 30 μ L aluminum pans with heating and cooling rates of 5 K/min under an N₂ stream; peak temperatures are given in Tables 1.

X-ray diffraction: Identification of the phase type and determination of the lattice parameters were carried out by small and wide-angle X-ray diffraction (XRD, Rigaku Co., Tokyo, Japan) on a temperature-controlled heating stage. Analysis was conducted on a D/max-3B spectrometer with Cu K α radiation.

Electron density reconstruction: Experimental diffractograms are fitted using Jade 6.0 to determine the positions and intensities of the diffraction peaks. The diffraction peaks are indexed based on their peak positions, and the lattice parameters and the space groups are subsequently determined. Once the diffraction intensities are measured and the corresponding plane group is determined, 2D electron density maps can be reconstructed based on the general formula:

$$E(xy) = \sum_{hk} \text{sqrt}[I(hk)] \exp[i2\pi(hx+ky) + \phi_{hk}]$$

For the molecular structures considered in this work, the phase angle ϕ_{hk} can take up the values of 0 or π . The choice of a phase combination was initially made on the merit of each reconstructed electron density map obtained using the most intense reflections, combined with the additional knowledge of the molecules (molecular shape, length, volume of each part and the distribution of electron density among the different moieties).

Photophysical properties measurements: The UV-vis absorption and PL spectra were carried out on UV2600A UV-vis absorption spectrometer (UNICO, China) and Hitachi F-7000 fluorescence spectrometer (Hitachi, Japan).

The quantum yields of compounds in organic solvents were determined using quinolinium hydrogen sulphate in H₂SO₄ ($\Phi_F=0.55$) as standard and applying the following equation.^{S1}

$$\Phi_{F_x} = \Phi_{F_{st}} \frac{A_{st} F_x n_x^2}{A_x F_{st} n_{st}^2}$$

Φ_{F_x} = the quantum yields of the samples; $\Phi_{F_{st}}$ = the quantum yield of the standard; A = the absorbance of the solution; F = the integration of corrected fluorescence spectrum; n = the average refractive index of the solvent.

The luminous efficiencies (LE) of the LE-LCDs and WLEDs were measured using a fluorescence spectrometer (Hitachi F-7000) equipped with an integrating sphere at an applied current of 20 mA. The absolute quantum yields of the films were also tested in this spectrometer.

Theoretical calculation: Molecular models were built using Materials Studio 8.0 (Accelrys). Geometry optimization was performed using Gaussian 09 with B3LYP/6-31G (d) level.

Fabrication of LC device for the dichroic ratio experiment: Nematic LC SLC9023 and TEB300 were purchased from Energy Chemical. The planar oriented LC cells (cell gap: 4.8 μm) with a homogeneously rubbed polyimide (PI) alignment layer were purchased from SOOBOO INTL SHARES LIMETED (China). The LC mixtures were prepared by combining solutions of the SLC9023 + 0.5 wt % **F16** or TEB300 + 0.5 wt % **TF16** in dichloromethane. The resulting solutions were then sonicated for about 1 min in order to achieve good solution, and thereafter, dichloromethane was evaporated off completely. Then the LC mixtures were filled into the empty LC cell by capillary action. The polarized emission spectra of the mixture in LC cell were measured by Hitachi F-7000 fluorescence spectrometer (Hitachi, Japan) with a polarization unit (P/N 250-2420). Notably, please make sure the rubbing direction of the LC cell is parallel to the analyzer. After we get the fluorescence intensity for parallel irradiation ($F_{//}$) and the fluorescence intensity for perpendicular irradiation (F_{\perp}), the dichroic ratio (N_F) was determined from the formula: $N_F = F_{//}/F_{\perp}$.

Fabrication of LC device with patterned electrode: Firstly, two clean LC glass substrates were prepared. One has patterned ITO and the other one has uniform ITO. After that, the LC cell was fabricated according to the above method. The prepared LC cell was connected with electric field power supply. To test the performance of the device, the structure shown in **Fig. 14** was used. In the structure, a 365 nm UV lamp was used as the light source to illuminate the mixture material.

Fabrication organic/n-Si heterojunction solar cell

Materials and precursor solution preparation: One-side polished n-type Si wafers (Resistivity: 0.05-0.1 Ω cm; thickness: 300 μm) was purchased from Hefei kejing materials Technology Corp. PEDOT:PSS (4083) aqueous solution was purchased from Xi'an Polymer light Technology Corp. PEDOT:PSS (Clevios PH1000) aqueous solution was purchased from Heraeus. For adjusting the electrical properties of the PEDOT:PSS films, PEDOT:PSS aqueous solution was added with mass ratio of DMSO 5 wt %. To adjust the wettability of the PEDOT:PSS pristine solution, mass ratios of surfactant Triton X-100 0.2 wt % were added to the pristine solution, and the mass ratios of **F18** 1.1 wt % or **TF18** 0.8 wt % THF solution were added to the precursor solution, and then ultrasonically shook for 24 hours.

Characterization of the PEDOT:PSS film: One-side polished n-type Si wafers was used to fabricate modified PEDOT:PSS films for Characterization and PEDOT:PSS:LC/n-Si solar cell. The Si wafers were cleaned with a standard RCA process to obtain clean and smooth Si substrates. Then, the Si substrates were dipped into a dilute hydrofluoric acid solution (10 wt %) for one minute to remove native oxide. The electrical characteristic of the PEDOT:PSS films on the quartz glass was measured by Hall measurement system (East Changing, HT-100). Hall effect measurement was performed using a vanderborg test geometry, the hall measurement devices were fabricated on a 1-mm-thick quartz glass substrate that was pre-cleaned by sonication in deionized water, acetone and

ethanol. The Ag (1 mm², 100 nm) electrodes were thermally evaporated through a shadow mask to form a channel length and channel width of 8 mm.

Device fabrication and characterization: The additive PEDOT:PSS solution was first spin-coated on the 1 cm² cleaned Si wafer with a spin-speed of 2500~3000 rpm for 40 s and annealing at 130 °C for 30 min. The spin-speed is used to control the thickness of PEDOT:PSS film to minimize light reflection from devices. After all of that, the Si substrates were transferred into the high vacuum evaporation system, and the 200 nm thick Ag-grid front electrodes and 100 nm thick Al rear electrode were deposited by thermal evaporation under vacuum condition (5.0×10^{-6} mbar). The Ag-grid consists of a main grid and seven fine grids. The length of the fine grid is 10 mm. The width of the main grid is 0.2 mm, and the width of the fine grid is 0.1 mm. The total coverage area of Ag-grid is 9 % of the solar cell. The current density-voltage (J - V) of PEDOT:PSS/n-Si solar cells was measured by employing Keithley 2400 under a simulated 100 mW/cm² solar illumination (AM 1.5 Global solar simulator), and the intensity was calibrated by a standard mono-crystalline silicon solar cell (PV measurements).

1.2 Additional textures and DSC traces

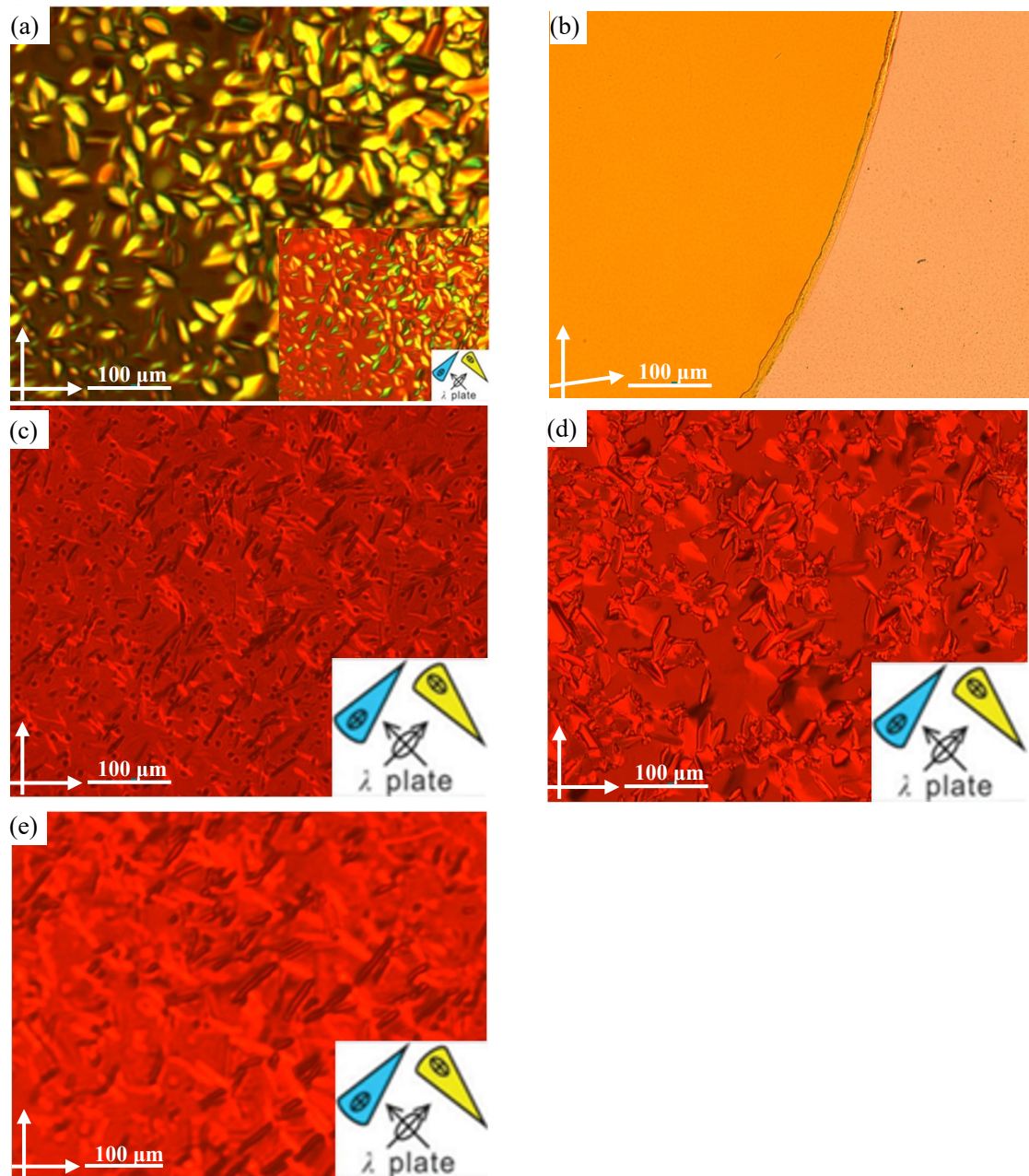


Fig. S1 Polarizing optical microscopy textures of the $\text{Col}_{\text{hex}}/p6mm$, $\text{Col}_{\text{squ}}/p4mm$ and $\text{Cub}/Pm\bar{3}n$ phases. (a) fan-like texture of the $\text{Col}_{\text{hex}}/p6mm$ phase of **F12** at 120 °C, inset shows texture with a λ -retarder plate; (b) texture of the $\text{Cub}/Pm\bar{3}n$ phase of **F22** at 120 °C. (c-e) the texture with additional λ -retarder plate indicating negative sign of the birefringence of **TFn**. (c) the $\text{Col}_{\text{hex}}/p6mm$ phase of **TF16** at 120 °C; (d) the $\text{Col}_{\text{hex}}/p6mm$ phase of **TF18** at 130 °C; (e) the $\text{Col}_{\text{squ}}/p4mm$ phase of **TF22** at 110 °C.

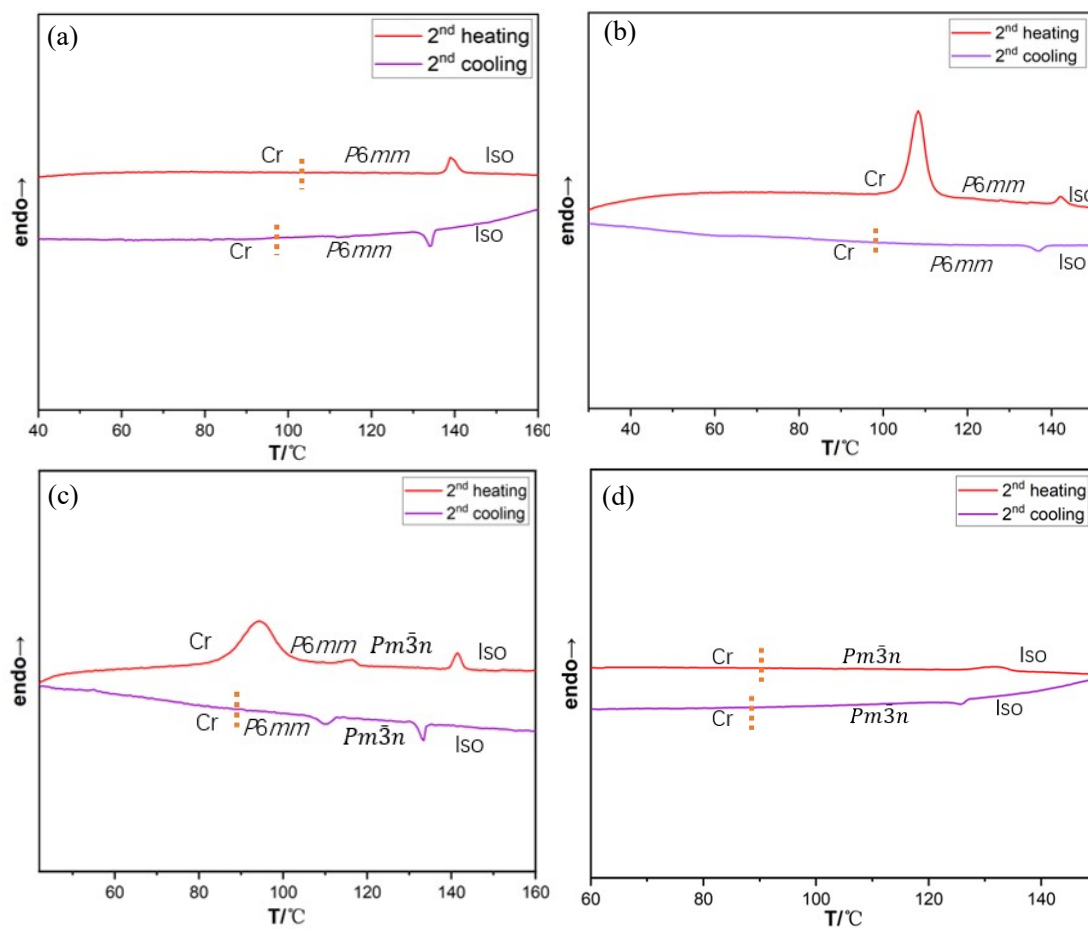


Fig. S2 DSC heating and cooling scans (5 K min⁻¹) of compounds **F12** (a), **F16** (b), **F18** (c) and **F22** (d). Red line represents heating process, purple line represents cooling process.

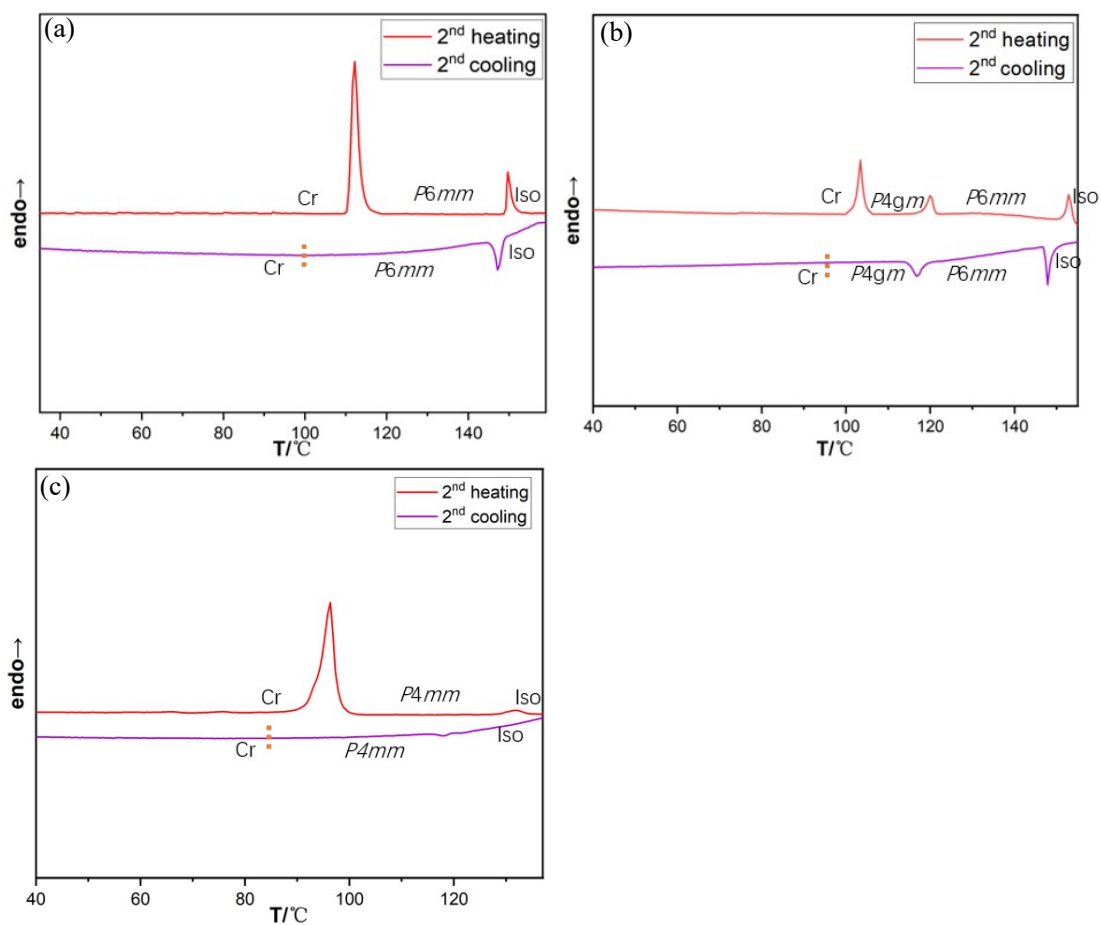


Fig. S3 DSC heating and cooling scans (5 K min⁻¹) of compounds **TF16** (a), **TF18** (b) and **TF22** (c). Red line represents heating process, purple line represents cooling process.

1.3 Additional XRD data

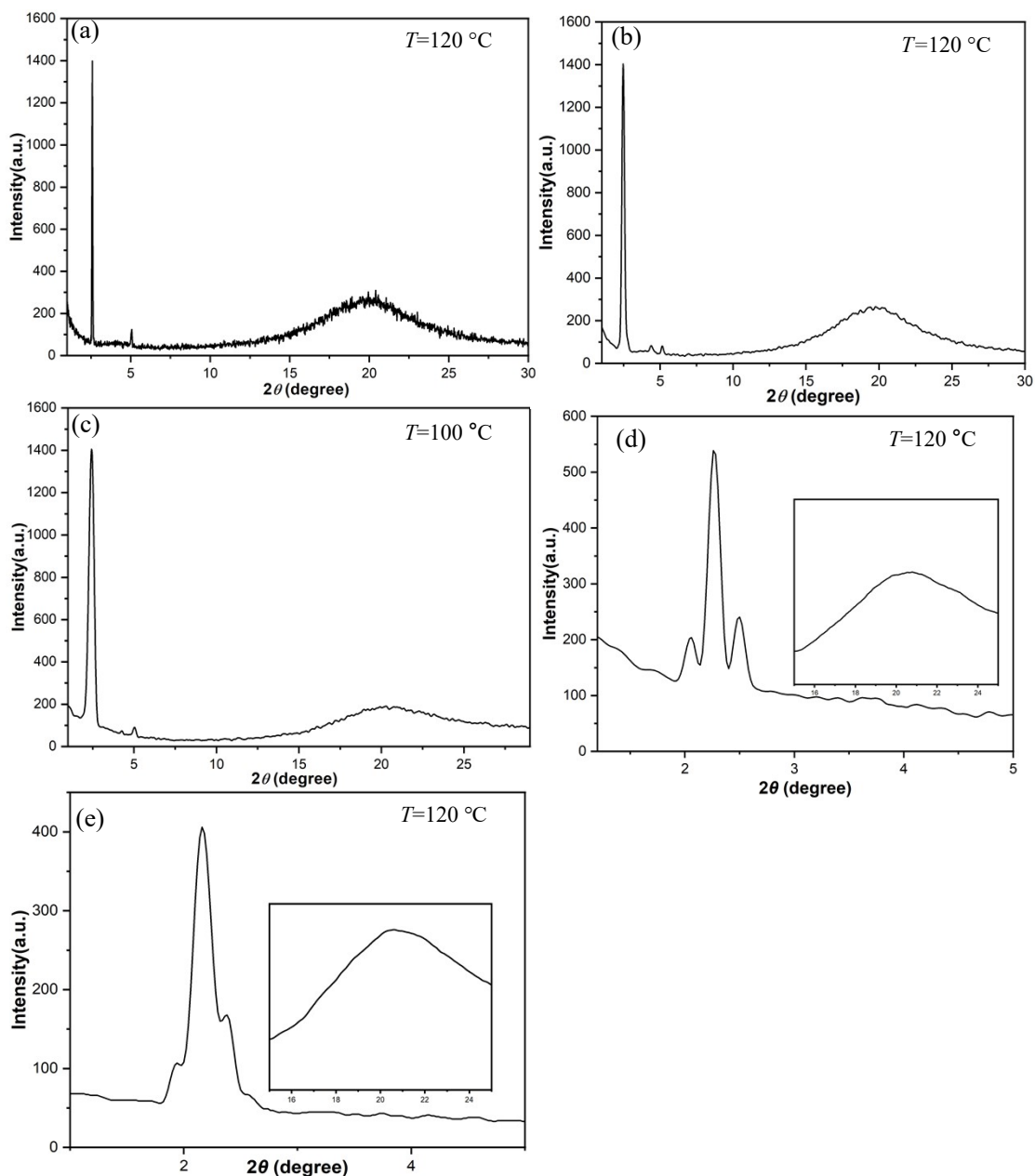


Fig. S4 XRD patterns of the $Col_{hex}/p6mm$ phase of compounds **F12** (a), **F16** (b) and **F18** (c); XRD patterns of the $Cub/Pm\bar{3}n$ phase of compounds **F18** (d) and **F22** (e).

Table S1 Experimental and calculated d -spacings and relative integrated intensities, for the $Col_{hex}/p6mm$ phase of **F12** at $120\text{ }^{\circ}\text{C}$. All intensities values are Lorentz corrected with correction for multiplicity.

$(hk)^a$	$2\theta_{obs.} (^{\circ})$	$d_{obs.} \text{-spacing}(\text{nm})$	$d_{cal.} \text{-spacing}(\text{nm})$	Intensity
10	2.58	3.42	3.45	100
11	4.43	1.99	1.99	0.3
20	5.08	1.74	1.72	8.9
$a_{hex} = 3.98\text{ nm}$				

^a (hk) : assigned indices for 2D phases.

Table S2 Experimental and calculated d -spacings and relative integrated intensities, for the $\text{Col}_{\text{hex}}/p6mm$ phase of **F16** at 120 °C. All intensities values are Lorentz corrected with correction for multiplicity.

(hk)	$2\theta_{\text{obs.}} (^\circ)$	$d_{\text{obs.}}\text{-spacing}(\text{nm})$	$d_{\text{cal.}}\text{-spacing}(\text{nm})$	<i>Intensity</i>
10	2.46	3.59	3.51	100
11	4.28	2.06	2.05	5.9
20	5.04	1.75	1.78	5.7
$a_{\text{hex}}=4.10 \text{ nm}$				

Table S3 Experimental and calculated d -spacings and relative integrated intensities, for the $\text{Col}_{\text{hex}}/p6mm$ phase of **F18** at 100 °C. All intensities values are Lorentz corrected with correction for multiplicity.

(hk)	$2\theta_{\text{obs.}} (^\circ)$	$d_{\text{obs.}}\text{-spacing}(\text{nm})$	$d_{\text{cal.}}\text{-spacing}(\text{nm})$	<i>Intensity</i>
10	2.44	3.61	3.59	100
11	4.22	2.09	2.08	2.3
20	4.96	1.78	1.80	6.5
$a_{\text{hex}}=4.15 \text{ nm}$				

Table S4 Experimental and calculated d -spacings and relative integrated intensities, for the $\text{Cub}/Pm\bar{3}n$ phase of **F18** at 120 °C. All intensities values are Lorentz corrected with correction for multiplicity.

$(hkl)^a$	$2\theta_{\text{obs.}} (^\circ)$	$d_{\text{obs.}}\text{-spacing}(\text{nm})$	$d_{\text{cal.}}\text{-spacing}(\text{nm})$	<i>Intensity</i>
(200)	2.05	4.31	4.30	37.9
(210)	2.28	3.87	3.85	100
(211)	2.52	3.49	3.52	44.6
$a_{\text{cub}}=8.61 \text{ nm}$				

^a (hkl) : assigned indices for 3D phase.

Table S5 Experimental and calculated d -spacings and relative integrated intensities, for the $\text{Cub}/Pm\bar{3}n$ phase of **F22** at 120 °C. All intensities values are Lorentz corrected with correction for multiplicity.

(hkl)	$2\theta_{\text{obs.}} (^\circ)$	$d_{\text{obs.}}\text{-spacing}(\text{nm})$	$d_{\text{cal.}}\text{-spacing}(\text{nm})$	<i>Intensity</i>
(200)	1.93	4.58	4.55	26.3
(210)	2.17	4.07	4.07	100
(211)	2.36	3.73	3.72	40.5
$a_{\text{cub}}=9.10 \text{ nm}$				

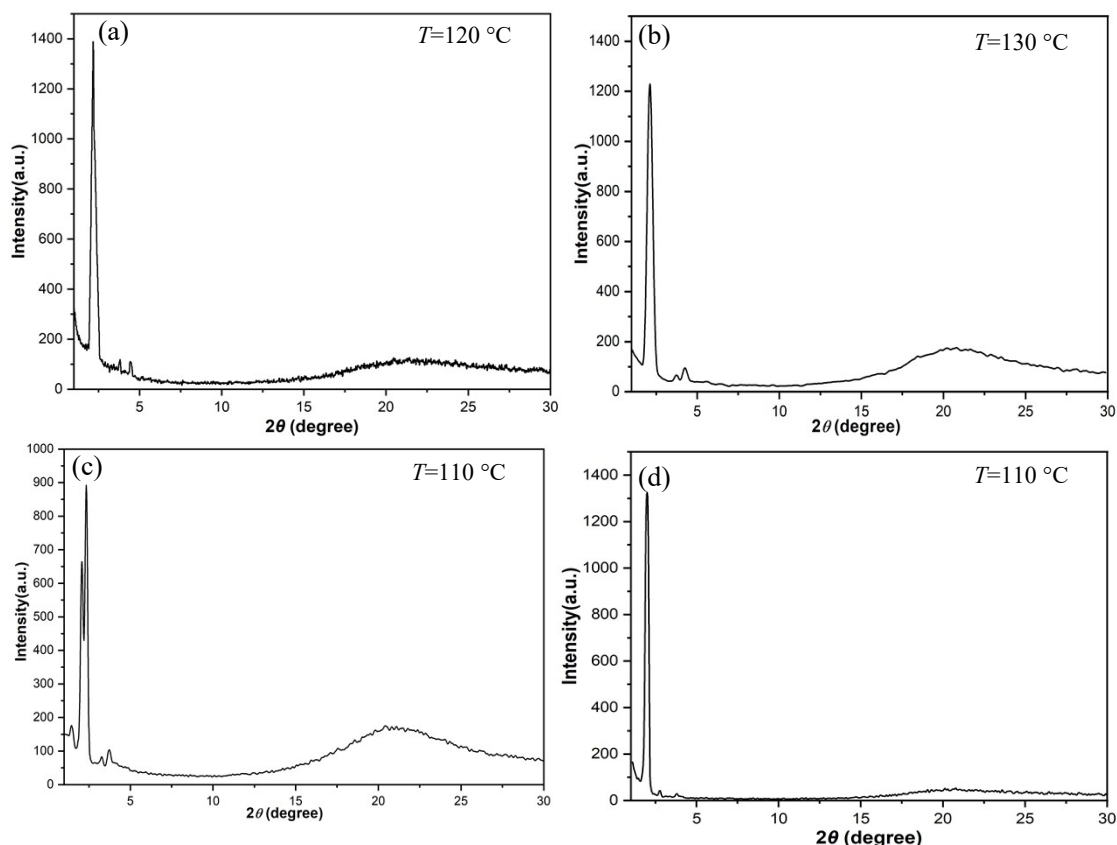


Fig. S5 XRD patterns of the Col_{hex}/p6mm phase of compounds **TF16** (a) and **TF18** (b); (c) XRD patterns of the Col_{squ}/p4gm phase of compound **TF18**; (d) XRD patterns of the Col_{squ}/p4mm phase of compound **TF22**.

Table S6 Experimental and calculated *d*-spacings and relative integrated intensities, for the Col_{hex}/p6mm phase of **TF16** at 120 °C. All intensities values are Lorentz corrected with correction for multiplicity.

(<i>hk</i>)	$2\theta_{\text{obs.}} (^{\circ})$	$d_{\text{obs.}}\text{-spacing}(\text{nm})$	$d_{\text{cal.}}\text{-spacing}(\text{nm})$	<i>Intensity</i>
10	2.18	4.05	4.04	100
11	3.74	2.36	2.34	8.5
20	4.42	2.00	2.02	7.9
$a_{\text{hex}} = 4.67 \text{ nm}$				

Table S7 Experimental and calculated *d*-spacings and relative integrated intensities, for the Col_{squ}/p4gm phase of **TF18** at 110 °C. All intensities values are Lorentz corrected with correction for multiplicity.

(<i>hk</i>)	$2\theta_{\text{obs.}} (^{\circ})$	$d_{\text{obs.}}\text{-spacing}(\text{nm})$	$d_{\text{cal.}}\text{-spacing}(\text{nm})$	<i>Intensity</i>
11	1.44	6.09	6.11	20.1
20	2.04	4.32	4.33	74.4
21	2.30	3.84	3.87	100
31	3.22	2.74	2.73	9.3
32	3.68	2.40	2.40	11.7
$a_{\text{squ}} = 8.65 \text{ nm}$				

Table S8 Experimental and calculated d -spacings and relative integrated intensities, for the $\text{Col}_{\text{hex}}/p6mm$ phase of **TF18** at 130 °C. All intensities values are Lorentz corrected with correction for multiplicity.

(hk)	$2\theta_{\text{obs.}} (^\circ)$	$d_{\text{obs.}}\text{-spacing}(\text{nm})$	$d_{\text{cal.}}\text{-spacing}(\text{nm})$	<i>Intensity</i>
10	2.14	4.12	4.10	100
11	3.74	2.36	2.37	5.2
20	4.30	2.05	2.05	7.7
$a_{\text{hex}} = 4.74 \text{ nm}$				

Table S9 Experimental and calculated d -spacings and relative integrated intensities, for the $\text{Col}_{\text{hex}}/p4mm$ phase of **TF22** at 110 °C. All intensities values are Lorentz corrected with correction for multiplicity.

(hk)	$2\theta_{\text{obs.}} (^\circ)$	$d_{\text{obs.}}\text{-spacing}(\text{nm})$	$d_{\text{cal.}}\text{-spacing}(\text{nm})$	<i>Intensity</i>
10	1.96	4.50	4.49	100
11	2.82	3.13	3.17	3.2
20	3.88	2.27	2.25	2.2
$a_{\text{squ}} = 4.49 \text{ nm}$				

Table S10. Structural data for LC phases of compounds **F n** and **TF n** .

Comp.	phase	a/nm	$V_{\text{cell}}/\text{nm}^3$	$V_{\text{mol}}/\text{nm}^3$	n_{cryst}	n_{liq}	n_{cell}	n_{wall} (n_{bundle})
F12	$\text{Col}_{\text{hex}}/p6mm^a$	3.98	6.17	1.51	4.09	3.21	3.65	1.2
F16	$\text{Col}_{\text{hex}}/p6mm^a$	4.10	6.55	1.91	3.43	2.70	3.07	1.0
F18	$\text{Col}_{\text{hex}}/p6mm^a$	4.15	6.71	2.11	3.18	2.50	2.84	0.9
F18	$\text{Cub}/Pm\bar{3}nb$	8.61	638	2.11	302	237	269	5.0
F22	$\text{Cub}/Pm\bar{3}nb$	9.10	754	2.41	313	246	279	5.2
TF12	Cr	-	-	-	-	-	-	-
TF16	$\text{Col}_{\text{hex}}/p6mm^a$	4.67	8.50	2.05	4.15	3.26	3.71	1.2
TF18	$\text{Col}_{\text{squ}}/p4gm^c$	8.65	33.67	2.25	14.96	11.76	13.36	1.3
TF18	$\text{Col}_{\text{hex}}/p6mm^a$	4.74	8.76	2.25	3.89	3.06	3.47	1.2
TF22	$\text{Col}_{\text{squ}}/p4mm^c$	4.49	9.07	2.65	3.42	2.69	3.05	1.5

^a $V_{\text{cell}} = a^2 \times \sin(60^\circ) \times h$ where h represents the height of the unit cell and is assumed to be 0.45 nm. V_{mol} = volume of the molecule as determined by the crystal volume increments^{S2} n_{cryst} = number of molecules per unit cell in the crystalline state, calculated according to $n_{\text{cyst}} = V_{\text{cell}}/V_{\text{mol}}$ (average packing coefficient in the crystal is $k = 0.7$). n_{liq} = the number of molecules in the unit cell of an isotropic liquid with an average packing coefficient $k = 0.55$, calculated according to $n_{\text{liq}} = 0.55/0.7$. n_{cell} = number of molecules in the unit cell in the LC state as estimated from the average of n_{cryst} and n_{liq} . n_{wall} = number of molecules in the cross section of the honeycomb walls as $n_{\text{wall}} = n_{\text{cell}}/3$.

^b V_{cell} = volume of the unit cell, calculated according to $V_{\text{cell}} = a^3_{\text{cub}}$ n_{bundle} = number of molecules per bundle in the cubic organization as $n_{\text{bundle}} = n_{\text{cell}}/54$.

^c V_{cell} was determined according to $V_{\text{cell}} = a^2_{\text{squ}} h$ for the square, where h represents the height of the unit cell which was assumed to be 0.45 nm. n_{wall} = the number of molecules in the cross-section of the honeycomb walls, calculated as $n_{\text{wall}} = n_{\text{cell}}/10$ for $p4gm$ cells, $n_{\text{wall}} = n_{\text{cell}}/2$ for $p4mm$ cells.

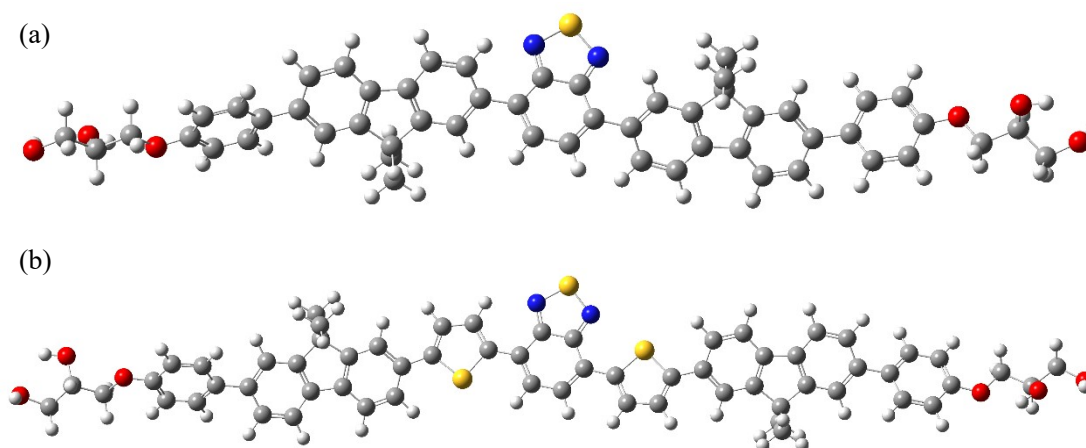


Fig. S6 Optimized structures of **Fn** (a) and **TFn** (b) were calculated at the B3LYP/6-31G(d) level by the DFT approach, where the lateral chains are replaced by methyl groups.

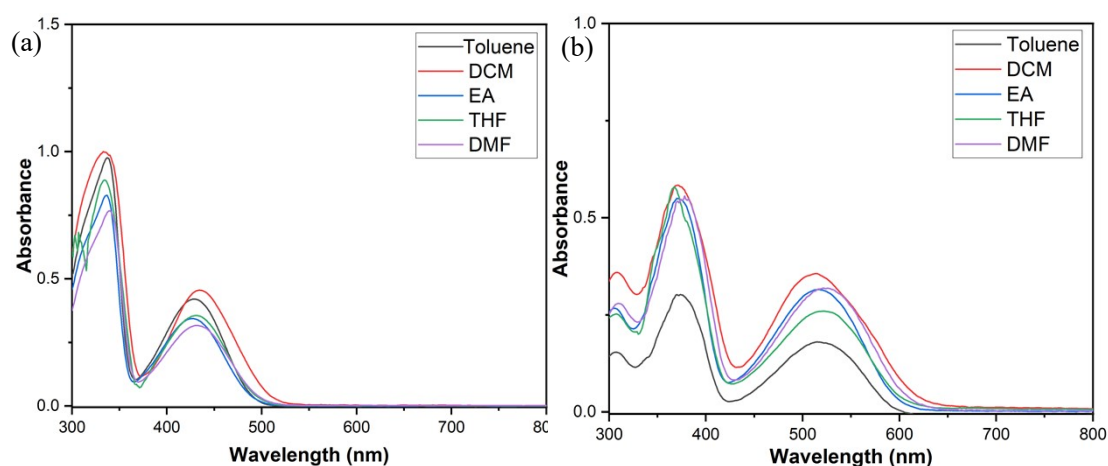
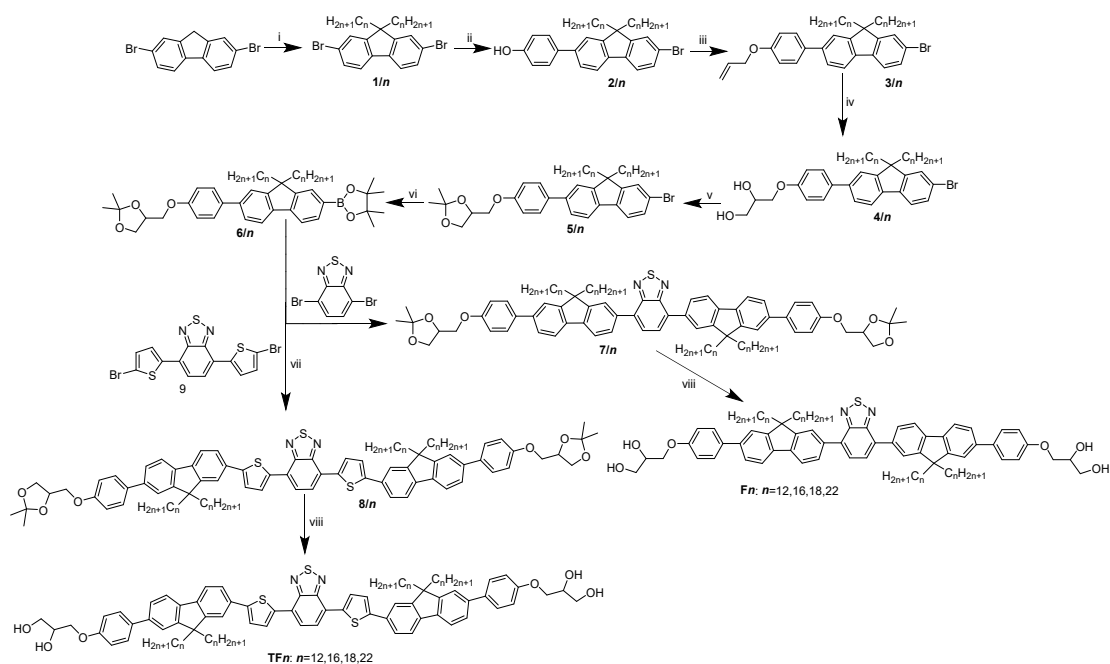


Fig. S7 Absorption spectra of **F16** (a) and **TF16** (b) in different organic solvents (10^{-5} M).

2. Material synthesis and analytical data

2.1 General remarks

The structures of the compounds are shown in Scheme S1. Reactions requiring an inert gas atmosphere were conducted under nitrogen and the glassware was oven-dried ($120\text{ }^{\circ}\text{C}$). Tetrahydrofuran (THF) was distilled from sodium prior to use. Commercially available chemicals were used as received. ^1H NMR and ^{13}C NMR spectra were recorded on a Bruker-DRX-400 (600) spectrometer. Thin-layer chromatography was performed on aluminum plates precoated with 5735 silica gel 60 PF254 (Merck). Column chromatography was performed on Merck silica gel 60 (300-400 mesh). Mass spectra were recorded with a Bruker rapifleX MALDI-TOF/TOF. The melting points (m.p.) of solid intermediates were determined by melting point meter (Jiahang JH30, China).



Scheme S1. Synthesis of **Fn** and **TFn**. Reagents and conditions: (i) $C_nH_{2n+1}Br$, *t*-BuOK, THF, 0 °C, 3 h; (ii) 4-hydroxyphenylboronic acid, Pd(PPh₃)₄, K₂CO₃, H₂O, THF, N₂, 78 °C, 12 h; (iii) K₂CO₃, CH₃CN, allyl bromide, 80 °C, 6 h; (iv) OsO₄, *N*-methylmorpholine *N*-oxide (NMMO, 60% aqueous solution), acetone, 50 °C, 5 h; (v) 2,2-dimethoxypropane, pyridinium *p*-toluene sulfonate (PPTS), THF, RT, 5 h; (vi) bis(pinacolato)diboron, PdCl₂(dppf), CH₃COOK, 1,4-dioxane, N₂, 100 °C, 12 h; (vii) Pd(PPh₃)₄, K₂CO₃, H₂O, THF, N₂, 78 °C, 15 h; (viii) 10% HCl, MeOH/THF, 75 °C, 6 h.

Compound 4,7-bis(5-bromothiophen-2-yl)benzo[*c*][1,2,5]thiadiazole (**9**)^{S3} was synthesized according to the references and the corresponding NMR data is consistent with those reported in reference.

Synthesis of 1/*n*

To an ice-cooled solution of 2,7-dibromofluorene (1 g, 3.11 mmol) in THF (30 mL) *tert*-BuOK (0.78 g, 7 mmol) was added and then the solution was stirred at room temperature for 15 min. 1-bromoalkane (6.84 mmol) was added dropwise into the solution, and the reaction mixture was continued to stir for additional 3 h. The reaction mixture was neutralized with 5% aqueous HCl solution (40 mL). After the reaction mixture was extracted with CH₂Cl₂ (3 × 25 mL). The combined organic layers were washed with water (3 × 25 mL). After drying over anhydrous MgSO₄, filtration and evaporation of the solvent, the residue was purified by column chromatography (eluent: petroleum ether).

1/12, Yield: 1.97 g, 96 %; white solid; m.p. 28-31 °C: ¹H NMR (CDCl₃, 400 MHz), δ (ppm): 7.53-7.51 (d, *J*=8.0 Hz, 2H, 2Ar-**H**), 7.46 (s, 2H, 2Ar-**H**), 7.46-7.44 (d, *J*=7.6 Hz, 2H, 2Ar-**H**), 1.92 (m, 4H, 2Ar-CH₂), 1.29 (m, 36H, 18CH₂), 0.88 (t, 6H, 2CH₃), 0.50 (m, 4H, 2CH₂);

1/16, Yield: 2.28 g, 95 %; white solid; m.p. 48-50 °C: ¹H NMR (CDCl₃, 400 MHz), δ (ppm): 7.53-7.51 (d, *J*=7.8 Hz, 2H, 2Ar-**H**), 7.46 (s, 2H, 2Ar-**H**), 7.46-7.44 (d, *J*=8.0 Hz, 2H, 2Ar-**H**), 1.93 (m, 4H, 2-ArCH₂), 1.29 (m, 52H, 26CH₂), 0.89 (t, 6H, 2CH₃), 0.49 (m, 4H, 2CH₂);

1/18, Yield: 2.45 g, 95 %; white solid; m.p. 60-63 °C: ¹H NMR (CDCl₃, 400 MHz), δ (ppm): 7.53-7.50 (d, *J*=8.4 Hz, 2H, 2Ar-H), 7.45 (s, 2H, 2Ar-H), 7.44-7.42 (d, *J*=7.6 Hz, 2H, 2Ar-H), 1.91 (m, 4H, 2ArCH₂), 1.24 (m, 60H, 30CH₂), 0.87 (t, 6H, 2CH₃), 0.47 (m, 4H, 2CH₂);

1/22, Yield: 2.8 g, 96 %; white solid; m.p. 71-73 °C: ¹H NMR (CDCl₃, 400 MHz), δ (ppm): 7.51-7.49 (d, *J*=8.0 Hz, 2H, 2Ar-H), 7.46 (s, 2H, 2Ar-H), 7.44-7.42 (d, *J*=8.4 Hz, 2H, 2Ar-H), 1.93 (m, 4H, 2-ArCH₂), 1.27 (m, 76H, 38CH₂), 0.88 (t, 6H, 2CH₃), 0.46 (m, 4H, 2CH₂).

Synthesis of 2/*n*

A mixture of 4-hydroxyphenylboronic acid (346 mg, 2.5 mmol), **1/*n*** (2.5 mmol), Pd(PPh₃)₄ (catalytic amount), THF (25 mL) and K₂CO₃ solution (10 mmol in 10 mL water) was stirred under N₂ atmosphere at reflux for 12 h. After cooling to room temperature, the solvent was removed and the residue was extracted with CH₂Cl₂ (3 × 25 mL). The combined organic layers were washed with water (3 × 25 mL). After drying over anhydrous MgSO₄, filtration and evaporation of the solvent. The residue was purified by column chromatography (eluent: petroleum ether: ethyl acetate = 10: 1).

2/12, Yield: 1.43 g, 85 %; viscous colorless liquid: ¹H NMR (CDCl₃, 400 MHz), δ (ppm): 7.70-7.68 (d, *J*=8.4 Hz, 1H, 1Ar-H), 7.56-7.52 (m, 4H, 4Ar-H), 7.51-7.49 (d, *J*=8.0 Hz, 2H, 2Ar-H), 7.46-7.44 (d, *J*=7.4 Hz, 1H, 1Ar-H), 6.95-6.93 (d, *J*=8.0 Hz, 2H, 2Ar-H), 4.80 (s, 1H, OH), 1.95 (m, 4H, 2Ar-2CH₂), 1.41 (m, 36H, 18CH₂), 0.88 (t, 6H, 2CH₃), 0.53 (m, 4H, 2CH₂);

2/16, Yield: 1.63 g, 83 %; viscous colorless liquid: ¹H NMR (CDCl₃, 400 MHz), δ (ppm): 7.70-7.68 (d, *J*=8.0 Hz, 1H, 2Ar-H), 7.56-7.53 (m, 4H, 4Ar-H), 7.52-7.50 (d, *J*=8.0 Hz, 2H, 2Ar-H), 7.46-7.44 (d, *J*=7.2 Hz, 1H, 1Ar-H), 6.95-6.93 (d, *J*=8.0 Hz, 2H, 2Ar-H), 4.81 (s, 1H, OH), 2.02 (m, 4H, 2Ar-2CH₂), 1.31 (m, 52H, 26CH₂), 0.89 (t, 6H, 2CH₃), 0.50 (m, 4H, 2CH₂);

2/18, Yield: 1.68 g, 80 %; viscous colorless liquid: ¹H NMR (CDCl₃, 400 MHz), δ (ppm): 7.71-7.69 (d, *J*=8.0 Hz, 1H, 1Ar-H), 7.56-7.51 (m, 4H, 4Ar-H), 7.51-7.49 (d, *J*=8.0 Hz, 2H, 2Ar-H), 7.46-7.44 (d, *J*=8.0 Hz, 1H, 1Ar-H), 6.95-6.93 (d, *J*=7.8 Hz, 2H, 2Ar-H), 4.83 (s, 1H, OH), 1.94 (m, 4H, 2Ar-CH₂), 1.35 (m, 60H, 30CH₂), 0.89 (t, 6H, 2CH₃), 0.51 (m, 4H, 2CH₂);

2/22, Yield: 1.88 g, 78 %; viscous colorless liquid: ¹H NMR (CDCl₃, 400 MHz), δ (ppm): 7.71-7.69 (d, *J*=8.0 Hz, 1H, 1Ar-H), 7.55-7.52 (m, 4H, 4Ar-H), 7.52-7.50 (d, *J*=8.0 Hz, 2H, 2Ar-H), 7.43-7.41 (d, *J*=7.6 Hz, 1H, 1Ar-H), 6.94-6.92 (d, *J*=8.0 Hz, 2H, 2Ar-H), 4.84 (s, 1H, OH), 1.97 (m, 4H, 2Ar-2CH₂), 1.33 (m, 76H, 38CH₂), 0.87 (t, 6H, 2CH₃), 0.53 (m, 4H, 2CH₂).

Synthesis of 3/*n*

A mixture of **2/*n*** (2 mmol), allyl bromide (363 mg, 3 mmol) and K₂CO₃ (680 mg, 5 mmol) in CH₃CN (30 mL) was stirred for 6 h under reflux. After cooling to room temperature, the reaction mixture was poured into ice-water (50 mL) and extracted with CH₂Cl₂ (3 × 25 mL). The combined organic layers were washed with water (3 × 25 mL). After drying over anhydrous MgSO₄, filtration and evaporation of the solvent. The crude product was purified by column chromatography (eluent:

petroleum ether: ethyl acetate = 10: 1).

3/12, Yield: 1.07 g, 75 %; colorless liquid: $^1\text{H NMR}$ (CDCl_3 , 400 MHz), δ (ppm): 7.70-7.68 (d, J = 8.0 Hz, 1H, Ar-**H**), 7.60-7.58 (d, J = 8.4 Hz, 2H, 2Ar-**H**), 7.57-7.54 (d, J = 8.4 Hz, 1H, Ar-**H**), 7.53 (m, 1H, Ar-**H**), 7.48 -7.47 (m, 1H, Ar-**H**), 7.46 (s, 1H, Ar-**H**), 7.45 (s, 1H, Ar-**H**), 7.05-7.00 (m, 2H, 2Ar-**H**), 6.13-6.05 (m, 1H, **CH=CH**₂), 5.46 (m, 1H, **CH=CH**₂), 5.32 (m, 1H, **CH=CH**₂), 4.60 (m, 2H, **OCH**₂), 2.03 (m, 4H, 2Ar-**CH**₂), 1.29 (m, 36H, 18**CH**₂), 0.90 (t, 6H, 2**CH**₃), 0.53 (m, 4H, 2**CH**₂);

3/16, Yield: 1.27 g, 77 %; colorless liquid: $^1\text{H NMR}$ (CDCl_3 , 400 MHz), δ (ppm): 7.70-7.68 (d, J = 8.0 Hz, 1H, Ar-**H**), 7.59-7.57 (d, J = 8.4 Hz, 2H, 2Ar-**H**), 7.57-7.54 (d, J = 8.4 Hz, 1H, Ar-**H**), 7.54 (m, 1H, Ar-**H**), 7.47 -7.45 (m, 1H, Ar-**H**), 7.45 (s, 1H, Ar-**H**), 7.44 (s, 1H, Ar-**H**), 7.04 -7.00 (m, 2H, 2Ar-**H**), 6.15-6.05 (m, 1H, **CH=CH**₂), 5.48 (m, 1H, **CH=CH**₂), 5.44 (m, 1H, **CH=CH**₂), 4.61 (m, 2H, **OCH**₂), 2.02 (m, 4H, 2Ar-**CH**₂), 1.31 (m, 52H, 26**CH**₂), 0.88 (t, 6H, 2**CH**₃), 0.49 (m, 4H, 2**CH**₂);

3/18, Yield: 1.23 g, 70 %; colorless liquid: $^1\text{H NMR}$ (CDCl_3 , 400 MHz), δ (ppm): 7.70-7.68 (d, J = 8.0 Hz, 1H, Ar-**H**), 7.59-7.57 (d, J = 8.0 Hz, 2H, 2Ar-**H**), 7.56-7.54 (d, J = 8.0 Hz, 1H, Ar-**H**), 7.54 (m 1H, Ar-**H**), 7.49 -7.48 (m, 1H, Ar-**H**), 7.47 (s, 1H, Ar-**H**), 7.44 (s, 1H, Ar-**H**), 7.07-7.02 (m, 2H, 2Ar-**H**), 6.14-6.05 (m, 1H, **CH=CH**₂), 5.46 (m, 1H, **CH=CH**₂), 5.43 (m, 1H, **CH=CH**₂), 4.62 (m, 2H, **OCH**₂), 2.10 (m, 4H, 2Ar-**CH**₂), 1.31 (m, 60H, 30**CH**₂), 0.89 (t, 6H, 2**CH**₃), 0.48 (m, 4H, 2**CH**₂);

3/22, Yield: 1.48 g, 80 %; colorless liquid: $^1\text{H NMR}$ (CDCl_3 , 400 MHz), δ (ppm): 7.72-7.70 (d, J = 8.4 Hz, 1H, Ar-**H**), 7.60-7.58 (d, J = 8.0 Hz, 2H, 2Ar-**H**), 7.57-7.55 (d, J = 8.0 Hz, 1H, Ar-**H**), 7.52 (m, 1H, Ar-**H**), 7.47-7.45 (m, 1H, Ar-**H**), 7.45 (s, 1H, Ar-**H**), 7.43 (s, 1H, Ar-**H**), 7.05-7.02 (m, 2H, 2Ar-**H**), 6.14-6.08 (m, 1H, **CH=CH**₂), 5.40 (m, 1H, **CH=CH**₂), 5.39 (m, 1H, **CH=CH**₂), 4.65 (m, 2H, **OCH**₂), 2.02 (m, 4H, 2 Ar-**CH**₂), 1.29 (m, 76H, 38**CH**₂), 0.89 (t, 6H, 2**CH**₃), 0.48 (m, 4H, 2**CH**₂).

Synthesis of 4/*n*

To a mixture of **3/*n*** (1 mmol) in acetone (20 mL) NMMO (2 mL, 60% solution in water) and OsO_4 (2.8 mL, 0.004 M solution in *tert*-butanol) was added. The mixture was stirred at 50 °C for 5 h and checked by TLC. After addition of saturated Na_2SO_3 solution in water (20 mL), the mixture was stirred for 1 h. The solution was diluted with water (50 mL) and extracted with ethyl acetate (3 × 20 mL). The combined organic layers were washed with water (3 × 25 mL). After drying over anhydrous MgSO_4 , filtration and evaporation of the solvent. The crude product was purified by column chromatography (eluent: dichloromethane: ethyl acetate = 15: 1).

4/12, Yield: 712 mg, 96 %; colorless liquid: $^1\text{H NMR}$ (CDCl_3 , 400 MHz), δ (ppm): 7.70-7.68 (d, J = 8.0 Hz, 1H, Ar- **H**), 7.60-7.57 (m, 2H, 2Ar-**H**), 7.54-7.52 (d, J = 8.4 Hz, 1H, Ar-**H**), 7.53-7.51 (d, J = 8.4 Hz, 1H, Ar-**H**), 7.47-7.45 (m, 2H, 2Ar-**H**), 7.45-7.43 (m, 1H, Ar-**H**), 6.98-6.95 (d, J = 8.4 Hz, 2H, 2Ar-**H**), 4.19 (m, 1H, HO-**CH**), 4.16 (m, 2H, HO-**CH**₂), 3.97 (m, 2H, O-**CH**₂), 1.95 (m, 4H, 2Ar-**CH**₂), 1.27 (m, 36H, 18**CH**₂), 0.87 (t, 6H, 2**CH**₃), 0.55 (m, 4H, 2**CH**₂);

4/16, Yield: 825 mg, 97 %; colorless liquid: $^1\text{H NMR}$ (CDCl_3 , 400 MHz), δ (ppm): 7.70-7.68 (d, J

= 7.6 Hz, 1H, Ar-**H**), 7.60-7.57 (m, 2H, 2Ar-**H**), 7.55-7.53 (d, $J = 8.0$ Hz, 1H, Ar-**H**), 7.53-7.51 (d, $J = 8.0$ Hz, 1H, Ar-**H**), 7.46-7.45 (m, 2H, 2Ar-**H**), 7.45-7.44 (m, 1H, Ar-**H**), 7.03-7.01 (d, $J = 8.8$ Hz, 2H, 2Ar-**H**), 4.15 (m, 1H, HO-**CH**), 4.12 (m, 2H, HO-**CH**₂), 3.91 (m, 2H, O-**CH**₂), 2.02 (m, 4H, 2Ar-**CH**₂), 1.30 (m, 52H, 26**CH**₂), 0.89 (t, 6H, 2**CH**₃), 0.50 (m, 4H, 2**CH**₂);

4/18, Yield: 870 mg, 95 %; colorless liquid: ¹H NMR (CDCl₃, 400 MHz), δ (ppm): 7.70-7.68 (d, $J = 8.0$ Hz, 1H, Ar-**H**), 7.60-7.57 (m, 2H, 2Ar-**H**), 7.55-7.53 (d, $J = 8.0$ Hz, 1H, Ar-**H**), 7.53-7.51 (d, $J = 8.0$ Hz, 1H, Ar-**H**), 7.47-7.45 (m, 2H, 2Ar-**H**), 7.45-7.43 (m, 1H, Ar-**H**), 6.97-6.95 (d, $J = 8.4$ Hz, 2H, 2Ar-**H**), 4.15 (m, 1H, HO-**CH**), 4.13 (m, 2H, HO-**CH**₂), 3.99 (m, 2H, O-**CH**₂), 1.91 (m, 4H, 2Ar-**CH**₂), 1.25 (m, 60H, 30**CH**₂), 0.89 (t, 6H, 2**CH**₃), 0.54 (m, 4H, 2**CH**₂);

4/22, Yield: 1.0 g, 97 %; colorless liquid: ¹H NMR (CDCl₃, 400 MHz), δ (ppm): 7.71-7.69 (d, $J = 7.6$ Hz, 1H, Ar-**H**), 7.63-7.56 (m, 2H, 2Ar-**H**), 7.55-7.53 (d, $J = 8.4$ Hz, 1H, Ar-**H**), 7.52-7.51 (d, $J = 7.4$ Hz, 1H, Ar-**H**), 7.50-7.46 (m, 2H, 2Ar-**H**), 7.42-7.39 (m, 1H, Ar-**H**), 6.95-6.93 (d, $J = 8.0$ Hz, 2H, 2Ar-**H**), 4.17 (m, 1H, HO-**CH**), 4.16 (m, 2H, HO-**CH**₂), 3.92 (m, 2H, O-**CH**₂), 1.98 (m, 4H, 2Ar-**CH**₂), 1.23 (m, 76H, 38**CH**₂), 0.89 (t, 6H, 2**CH**₃), 0.51 (m, 4H, 2**CH**₂).

Synthesis of **5/n**

A mixture of **4/n** (0.8 mmol), PPTS (20 mg) and 2,2-dimethoxypropane (40 mmol) in THF was stirred at room temperature for 5 h. Thereafter, the solvent was evaporated and the residue was taken up in ethyl acetate. The solution was washed with water (3 \times 25 mL). After drying over anhydrous MgSO₄, the solvent was removed under reduced pressure. The crude product was purified by column chromatography (eluent: petroleum ether/ethyl acetate = 15: 1).

5/12, Yield: 611 mg, 97 %; colorless liquid: ¹H NMR (CDCl₃, 400 MHz), δ (ppm): 7.69-7.67 (d, $J = 7.8$ Hz, 1H, Ar-**H**), 7.60-7.57 (m, 2H, 2Ar-**H**), 7.55-7.52 (m, 1H, Ar-**H**), 7.52-7.50 (m, 1H, Ar-**H**), 7.47-7.45 (m, 2H, 2Ar-**H**), 7.45-7.43 (m, 1H, Ar-**H**), 7.01-6.99 (d, $J = 8.7$ Hz, 2H, 2Ar-**H**), 4.53 (m, 1H, O-**CH**), 4.16 (m, 2H, O-**CH**₂), 3.97 (m, 2H, O-**CH**₂), 1.95 (m, 4H, 2Ar-**CH**₂), 1.57 (s, 6H, 2C-**CH**₃), 1.27 (m, 36H, 18**CH**₂), 0.87 (t, 6H, 2**CH**₃), 0.49 (m, 4H, 2**CH**₂);

5/16, Yield: 706 mg, 98 %; colorless liquid: ¹H NMR (CDCl₃, 400 MHz), δ (ppm): 7.70-7.68 (d, $J = 7.6$ Hz, 1H, Ar-**H**), 7.59-7.57 (m, 2H, 2Ar-**H**), 7.56-7.53 (m, 1H, Ar-**H**), 7.53-7.46 (m, 1H, Ar-**H**), 7.46-7.45 (m, 2H, 2Ar-**H**), 7.45-7.44 (m, 1H, Ar-**H**), 7.03-7.00 (d, $J = 8.8$ Hz, 2H, 2Ar-**H**), 4.55 (m, 1H, O-**CH**), 4.20 (m, 2H, O-**CH**₂), 4.12 (m, 2H, O-**CH**₂), 2.02 (m, 4H, 2Ar-**CH**₂), 1.57 (s, 6H, 2C-**CH**₃), 1.29 (m, 52H, 26**CH**₂), 0.89 (t, 6H, 2**CH**₃), 0.50 (m, 4H, 2**CH**₂);

5/18, Yield: 742 mg, 97 %; colorless liquid: ¹H NMR (CDCl₃, 400 MHz), δ (ppm): 7.71-7.69 (d, $J = 8.0$ Hz, 1H, Ar-**H**), 7.63-7.56 (m, 2H, 2Ar-**H**), 7.54-7.52 (m, 1H, Ar-**H**), 7.52-7.50 (m, 1H, Ar-**H**), 7.48-7.45 (m, 2H, 2Ar-**H**), 7.45-7.37 (m, 1H, Ar-**H**), 7.03-7.00 (d, $J = 8.8$ Hz, 2H, 2Ar-**H**), 4.50 (m, 1H, O-**CH**), 4.17 (m, 2H, O-**CH**₂), 3.94 (m, 2H, O-**CH**₂), 1.99 (m, 4H, 2Ar-**CH**₂), 1.57 (s, 6H, 2C-**CH**₃), 1.24 (m, 60H, 30**CH**₂), 0.84 (t, 6H, 2**CH**₃), 0.52 (m, 4H, 2**CH**₂);

5/22, Yield: 811 mg, 95 %; colorless liquid: ¹H NMR (CDCl₃, 400 MHz), δ (ppm): 7.67-7.65 (d, $J = 8.0$ Hz, 1H, Ar-**H**), 7.64-7.57 (m, 2H, 2Ar-**H**), 7.55-7.53 (m, 1H, Ar-**H**), 7.52-7.50 (m, 1H, Ar-**H**),

7.49-7.45 (m, 2H, 2Ar-H), 7.43-7.36 (m, 1H, Ar-H), 7.06-7.04 (d, $J = 8.6$ Hz, 2H, 2Ar-H), 4.55 (m, 1H, O-CH), 4.18 (m, 2H, O-CH₂), 3.90 (m, 2H, O-CH₂), 2.01 (m, 4H, 2Ar-CH₂), 1.54 (s, 6H, 2C-CH₃), 1.21 (m, 76H, 38CH₂), 0.90 (t, 6H, 2CH₃), 0.53 (m, 4H, 2CH₂).

Synthesis of 6/*n*

5/*n* (0.7 mmol), bis(pinacolato)diboron (1 mmol), CH₃COOK (490 mg, 5 mmol), and PdCl₂(dppf) (catalytic amount) were mixed in 1,4-dioxane (25 mL) under N₂ atmosphere and the mixture was heated at 100 °C for 12 h. After adding 50 mL of water to quench the reaction, the mixture was extracted with dichloromethane (3×25 mL). The combined organic layers were washed with water (3 × 25 mL). After drying over anhydrous MgSO₄, filtration and evaporation of the solvent, the crude product was purified by column chromatography (eluent: petroleum ether: ethyl acetate= 15:1).

6/12, Yield: 514 mg, 88 %; viscous colorless liquid: ¹H NMR (CDCl₃, 400 MHz), δ (ppm): 7.74-7.72 (d, $J = 8.0$ Hz, 1H, Ar-H), 7.70-7.68 (d, $J = 8.0$ Hz, 2H, 2Ar-H), 7.68-7.61 (m, 1H, Ar-H), 7.54-7.51 (m, 2H, 2Ar-H), 7.50-7.45 (m, 1H, Ar-H), 7.44-7.42 (m, 1H, 2Ar-H), 6.97-6.95 (d, $J = 8.0$ Hz, 2H, 2Ar-H), 4.45 (m, 1H, O-CH), 4.17 (m, 2H, O-CH₂), 3.93 (m, 2H, O-CH₂), 1.99 (m, 4H, 2Ar-CH₂), 1.35 (s, 12H, 4C-CH₃), 1.31 (s, 6H, 2C-CH₃), 1.20 (m, 36H, 18CH₂), 0.86 (t, 6H, 2CH₃), 0.54 (m, 4H, 2CH₂);

6/16, Yield: 597 mg, 90 %; viscous colorless liquid: ¹H NMR (CDCl₃, 400 MHz), δ (ppm): 7.75-7.73 (d, $J = 8.0$ Hz, 1H, Ar-H), 7.69-7.67 (d, $J = 8.4$ Hz, 2H, 2Ar-H), 7.67-7.62 (m, 1H, Ar-H), 7.53-7.51 (m, 2H, 2Ar-H), 7.51-7.46 (m, 1H, Ar-H), 7.44-7.42 (m, 1H, 2Ar-H), 6.96-6.94 (d, $J = 8.0$ Hz, 2H, 2Ar-H), 4.48 (m, 1H, O-CH), 4.15 (m, 2H, O-CH₂), 3.95 (m, 2H, O-CH₂), 1.98 (m, 4H, 2Ar-CH₂), 1.33 (s, 12H, 4C-CH₃), 1.30 (s, 6H, 2C-CH₃), 1.23 (m, 52H, 26CH₂), 0.82 (t, 6H, 2CH₃), 0.50 (m, 4H, 2CH₂);

6/18, Yield: 563 mg, 85 %; viscous colorless liquid: ¹H NMR (CDCl₃, 400 MHz), δ (ppm): 7.76-7.74 (d, $J = 8.0$ Hz, 1H, Ar-H), 7.71-7.69 (d, $J = 8.0$ Hz, 2H, 2Ar-H), 7.68-7.60 (m, 1H, Ar-H), 7.55-7.52 (m, 2H, 2Ar-H), 7.50-7.46 (m, 1H, Ar-H), 7.44-7.40 (m, 1H, 2Ar-H), 6.98-6.96 (d, $J = 8.4$ Hz, 2H, 2Ar-H), 4.47 (m, 1H, O-CH), 4.19 (m, 2H, O-CH₂), 3.90 (m, 2H, O-CH₂), 2.02 (m, 4H, 2Ar-CH₂), 1.34 (s, 12H, 4C-CH₃), 1.30 (s, 6H, 2C-CH₃), 1.97 (m, 60H, 30CH₂), 0.88 (t, 6H, 2CH₃), 0.52 (m, 4H, 2CH₂);

6/22, Yield: 624 mg, 80 %; viscous colorless liquid: ¹H NMR (CDCl₃, 400 MHz), δ (ppm): 7.74-7.72 (d, $J = 8.0$ Hz, 1H, Ar-H), 7.71-7.69 (d, $J = 8.0$ Hz, 2H, 2Ar-H), 7.68-7.62 (m, 1H, Ar-H), 7.55-7.51 (m, 2H, 2Ar-H), 7.50-7.46 (m, 1H, Ar-H), 7.45-7.41 (m, 1H, 2Ar-H), 6.99-6.97 (d, $J = 8.4$ Hz, 2H, 2Ar-H), 4.46 (m, 1H, O-CH), 4.16 (m, 2H, O-CH₂), 3.97 (m, 2H, O-CH₂), 1.97 (m, 4H, 2Ar-CH₂), 1.33 (s, 12H, 4C-CH₃), 1.31 (s, 6H, 2C-CH₃), 1.21 (m, 76H, 38CH₂), 0.88 (t, 6H, 2CH₃), 0.53 (m, 4H, 2CH₂);

Synthesis of 7/*n* and 8/*n*

A mixture of 4,7-dibromo-2,1,3-benzothiadiazole (29 mg, 0.1 mmol) or 4,7-bis(5-bromothiophen-2-yl)benzo[*c*][1,2,5]thiadiazole (**9**, 46 mg, 0.1 mmol), **6/*n*** (0.2 mmol), Pd(PPh₃)₄ (catalytic amount),

THF (20 mL) and K₂CO₃ solution (1 mmol in 5 mL water) was stirred under N₂ atmosphere at reflux for 15 h. After cooling to room temperature, the solvent was removed and the residue was extracted with CH₂Cl₂ (3 × 25 mL). The combined organic layers were washed with water (3 × 25 mL). After drying over anhydrous MgSO₄, the solvent was removed under reduced pressure, the crude product was used without further purification.

Synthesis of *Fn* and *TFn*

A mixture of the *7/n* or *8/n* (0.5 mmol) and 10% HCl (5 mL) was dissolved in THF/MeOH (1:1, 30 mL) and stirred at 75 °C for 6 h. After cooling to room temperature, the solvent was removed and the residue was extracted with CH₂Cl₂ (3 × 25 mL). The combined organic layers were washed with water (3 × 25 mL). After drying over anhydrous MgSO₄, the solvent was removed under reduced pressure. The product was purified by column chromatography (eluent: CHCl₃: MeOH= 9:1) and recrystallization from MeOH/THF.

F12, Yield: 101 mg, 69 %; yellow solid: ¹H NMR (400 MHz, CDCl₃) δ (ppm) 8.05-8.04 (d, *J* = 7.6 Hz, 2H, 2Ar-H), 7.97 (s, 2H, 2Ar-H), 7.90-7.87 (m, 4H, 4Ar-H), 7.82-7.80 (d, *J* = 7.6 Hz, 2H, 2Ar-H), 7.64-7.62 (d, *J* = 8.8 Hz, 4H, 4Ar-H), 7.58-7.56 (d, *J* = 8.4 Hz, 4H, 4Ar-H), 7.05-7.03 (d, *J* = 8.8 Hz, 4H, 4Ar-H), 4.18-4.12 (m, 6H, 2HO-CH₂, 2HO-CH), 3.91-3.78 (m, 4H, 2O-CH₂), 2.14-2.01 (m, 8H, 4Ar-CH₂), 1.25-1.10 (m, 72H, 36CH₂), 0.86-0.82 (m, 20H, 4CH₂CH₃). ¹³C NMR (100 MHz, CDCl₃) δ (ppm) 157.94, 154.38, 152.07, 151.35, 141.05, 139.74, 139.54, 136.12, 134.95, 133.58, 128.34, 128.24, 127.89, 125.72, 123.92, 121.19, 120.23, 119.72, 114.88, 70.43, 69.37, 63.69, 55.33, 40.35, 31.89, 30.10, 29.61, 29.32, 29.28, 23.96, 22.67, 14.11; HRMS, MALDI-TOF-MS *m/z*: Found 1470.0063 [M+H]⁺. Calculated For C₉₈H₁₃₆N₂O₆S: 1469.0119.

F16, Yield: 120 mg, 71 %; yellow solid: ¹H NMR (CDCl₃, 400 MHz), δ (ppm): 8.06-8.04 (d, *J* = 8.0 Hz, 2H, 2Ar-H), 7.97 (s, 2H, 2Ar-H), 7.90-7.87 (m, 4H, 4Ar-H), 7.82-7.80 (d, *J* = 8.0 Hz, 2H, 2Ar-H), 7.65-7.62 (d, *J* = 8.4 Hz, 4H, 4Ar-H), 7.58-7.55 (m, 4H, 4Ar-H), 7.05-7.03 (d, *J* = 8.8 Hz, 4H, 4Ar-H), 4.18-4.12 (m, 6H, 2HO-CH₂, 2HO-CH), 3.92-3.79 (m, 4H, 2O-CH₂), 2.14-2.01 (m, 8H, 4Ar-CH₂), 1.22-1.10 (m, 104H, 52CH₂), 0.88-0.85 (m, 20H, 4CH₂CH₃). ¹³C NMR (100 MHz, CDCl₃) δ (ppm) 157.94, 154.39, 152.07, 151.35, 141.05, 139.74, 139.54, 136.12, 134.96, 133.58, 128.35, 128.25, 127.89, 125.72, 123.92, 121.20, 120.23, 119.73, 114.88, 70.42, 69.38, 63.69, 55.34, 40.36, 31.93, 30.12, 29.68, 29.64, 29.36, 29.30, 23.98, 22.70, 14.13; HRMS, MALDI-TOF-MS *m/z*: Found 1694.2580 [M+H]⁺. Calculated For C₁₁₄H₁₆₈N₂O₆S: 1693.2623.

F18, Yield: 99 mg, 55 %; yellow solid: ¹H NMR (400 MHz, CDCl₃) δ (ppm) 8.06-8.04 (d, *J* = 8.0 Hz, 2H, 2Ar-H), 7.98 (s, 2H, 2Ar-H), 7.90-7.87 (m, 4H, 4Ar-H), 7.81-8.79 (d, *J* = 8.4 Hz, 2H, 2Ar-H), 7.65-7.63 (d, *J* = 8.8 Hz, 4H, 4Ar-H), 7.57-7.56 (m, 4H, 4Ar-H), 7.06-7.03 (d, *J* = 8.4 Hz, 4H, 4Ar-H), 4.19-4.12 (m, 6H, 2HO-CH₂, 2HO-CH), 3.92-3.78 (m, 4H, 2O-CH₂), 2.13-2.04 (m, 8H, 4Ar-CH₂), 1.24-1.10 (m, 120H, 60CH₂), 0.89-0.86 (m, 20H, 4CH₂CH₃). ¹³C NMR (100 MHz, CDCl₃) δ (ppm) 157.95, 154.37, 152.08, 151.35, 141.04, 139.72, 139.52, 136.11, 134.88, 133.56, 128.34, 128.25, 127.91, 125.72, 123.92, 121.17, 120.25, 119.75, 114.87, 70.50, 69.31, 63.69, 55.33, 40.36, 31.95, 30.13, 29.92, 29.72, 29.69, 29.39, 29.32, 29.04, 23.99, 22.72, 14.16; HRMS, MALDI-TOF-MS *m/z*: Found 1806.3827 [M+H]⁺. Calculated For C₁₂₂H₁₈₄N₂O₆S: 1805.3875.

F22, Yield: 101 mg, 50 %; yellow solid: ^1H NMR (400 MHz, CDCl_3) δ (ppm) 8.06-8.04 (d, $J = 8.0$ Hz, 2H, 2Ar-H), 7.97 (s, 2H, 2Ar-H), 7.90-7.87 (m, 4H, 4Ar-H), 7.82-7.80 (d, $J = 8.0$ Hz, 2H, 2Ar-H), 7.65-7.62 (d, $J = 8.8$ Hz, 4H, 4Ar-H), 7.58-7.56 (m, 4H, 4Ar-H), 7.05-7.03 (d, $J = 8.8$ Hz, 4H, 4Ar-H), 4.17-4.12 (m, 6H, 2HO- CH_2 , 2HO-CH), 3.91-3.80 (m, 4H, 2O- CH_2), 2.09-2.03 (m, 8H, 4Ar- CH_2), 1.24-1.10 (m, 152H, 76 CH_2), 0.89-0.83 (m, 20H, 4 CH_2CH_3). ^{13}C NMR (100 MHz, CDCl_3) δ (ppm) 157.93, 154.38, 152.07, 151.35, 141.04, 139.73, 139.54, 136.12, 134.95, 133.58, 128.35, 128.25, 127.90, 125.73, 123.91, 121.19, 120.23, 119.73, 114.87, 70.41, 69.36, 63.69, 55.33, 40.37, 31.95, 30.12, 29.72, 29.69, 29.66, 29.64, 29.39, 29.31, 23.97, 22.72, 14.15; HRMS, MALDI-TOF-MS m/z : Found 2030.6379 $[\text{M}+\text{H}]^+$. Calculated For $\text{C}_{138}\text{H}_{216}\text{N}_2\text{O}_6\text{S}$: 2029.6379.

TF12, Yield: 106 mg, 64 %; red solid: ^1H NMR (600 MHz, CDCl_3) δ (ppm) 8.16-8.16 (d, $J = 3.6$ Hz, 2H, 2Ar-H), 7.93 (s, 2H, 2Ar-H), 7.74-7.72 (m, 6H, 6Ar-H), 7.67 (s, 2H, 2Ar-H), 7.62-7.61 (d, $J = 8.4$ Hz, 4H, 4Ar-H), 7.54-7.53 (d, $J = 7.8$ Hz, 4H, 4Ar-H), 7.52-7.50 (d, $J = 12$ Hz, 2H, 2Ar-H), 7.04-7.02 (d, $J = 8.4$ Hz, 4H, 4Ar-H), 4.17-4.10 (m, 6H, 2HO- CH_2 , 2HO-CH), 3.90-3.79 (m, 4H, 2O- CH_2), 2.09-2.05 (m, 8H, 4Ar- CH_2), 1.27-1.07 (m, 72H, 36 CH_2), 0.87-0.84 (t, 12H, 4 CH_3), 0.73 (m, 8H, 4 CH_2CH_3). ^{13}C NMR (150 MHz, CDCl_3) δ (ppm) 157.95, 152.67, 151.85, 151.71, 146.49, 140.85, 139.67, 139.48, 138.33, 134.89, 132.83, 128.70, 128.32, 125.80, 125.72, 125.29, 124.86, 123.92, 121.09, 120.15, 120.07, 120.03, 114.89, 70.42, 69.37, 63.69, 55.36, 40.46, 31.94, 30.04, 29.70, 29.67, 29.66, 29.62, 29.60, 29.38, 29.27, 23.83, 22.71, 14.15; HRMS, MALDI-TOF-MS m/z : Found 1633.9893 $[\text{M}+\text{H}]^+$. Calculated For $\text{C}_{106}\text{H}_{140}\text{N}_2\text{O}_6\text{S}_3$: 1632.9874.

TF16, Yield: 125 mg, 67 %; red solid: ^1H NMR (400 MHz, CDCl_3) δ (ppm) 8.17-8.16 (d, $J = 3.6$ Hz, 2H, 2Ar-H), 7.93 (s, 2H, 2Ar-H), 7.74-7.72 (m, 6H, 6Ar-H), 7.68 (s, 2H, 2Ar-H), 7.63-7.61 (d, $J = 8.8$ Hz, 4H, 4Ar-H), 7.55-7.53 (d, $J = 8.0$ Hz, 4H, 4Ar-H), 7.52-7.50 (d, $J = 6.4$ Hz, 2H, 2Ar-H), 7.04-7.02 (d, $J = 8.8$ Hz, 4H, 4Ar-H), 4.18-4.11 (m, 6H, 2HO- CH_2 , 2HO-CH), 3.91-3.78 (m, 4H, 2O- CH_2), 2.08-2.04 (m, 8H, 4Ar- CH_2), 1.25-1.07 (m, 104H, 52 CH_2), 0.87-0.84 (t, 12H, 4 CH_3), 0.72 (m, 8H, 4 CH_2CH_3). ^{13}C NMR (100 MHz, CDCl_3) δ (ppm) 157.94, 152.66, 151.84, 151.70, 146.48, 140.84, 139.67, 139.47, 138.33, 134.88, 132.82, 128.69, 128.31, 125.80, 125.72, 125.28, 124.85, 123.91, 121.08, 120.14, 120.06, 120.03, 114.88, 70.41, 69.37, 63.68, 55.35, 40.45, 31.93, 30.03, 29.69, 29.67, 29.66, 29.62, 29.60, 29.37, 29.26, 25.62, 23.82, 22.70, 14.14; HRMS, MALDI-TOF-MS m/z : Found 1858.2391 $[\text{M}+\text{H}]^+$. Calculated For $\text{C}_{122}\text{H}_{172}\text{N}_2\text{O}_6\text{S}_3$: 1857.2378.

TF18, Yield: 118 mg, 60 %; red solid: ^1H NMR (600 MHz, CDCl_3) δ (ppm) 8.17-8.16 (d, $J = 3.6$ Hz, 2H, 2Ar-H), 7.94 (s, 2H, 2Ar-H), 7.74-7.71 (m, 6H, 6Ar-H), 7.68 (s, 2H, 2Ar-H), 7.62-7.61 (d, $J = 8.4$ Hz, 4H, 4Ar-H), 7.55-7.53 (d, $J = 7.8$ Hz, 4H, 4Ar-H), 7.52-7.50 (d, $J = 8$ Hz, 2H, 2Ar-H), 7.04-7.02 (d, $J = 9.0$ Hz, 4H, 4Ar-H), 4.17-4.12 (m, 6H, 2HO- CH_2 , 2HO-CH), 3.90-3.79 (m, 4H, 2HO- CH_2), 2.07-2.05 (m, 8H, 4Ar- CH_2), 1.28-1.07 (m, 120H, 60 CH_2), 0.88-0.85 (t, 12H, 4 CH_3), 0.73 (m, 8H, 4 CH_2CH_3). ^{13}C NMR (150 MHz, CDCl_3) δ (ppm) 157.93, 152.65, 151.82, 151.68, 146.47, 140.83, 139.65, 139.45, 138.31, 134.87, 132.80, 128.68, 128.30, 125.79, 125.70, 125.27, 124.84, 123.89, 121.07, 120.12, 120.03, 120.01, 114.86, 70.40, 69.35, 63.67, 55.33, 40.44, 31.92, 30.01, 29.69, 29.65, 29.64, 29.60, 29.58, 29.36, 29.24, 23.80, 22.69, 14.12; HRMA, MALDI-TOF-MS m/z : Found 1970.3666 $[\text{M}+\text{H}]^+$. Calculated For $\text{C}_{130}\text{H}_{188}\text{N}_2\text{O}_6\text{S}_3$: 1969.3630.

TF22, Yield: 125 mg, 57 %; red solid: ^1H NMR (400 MHz, CDCl_3) δ (ppm) 8.16-8.15(d, $J = 3.6$ Hz, 2H, 2Ar-H), 7.92 (s, 2H, 2Ar-H), 7.74-7.71 (m, 6H, 6Ar-H), 7.68 (s, 2H, 2Ar-H), 7.63-7.60 (d, $J = 8.8$ Hz, 4H, 4Ar-H), 7.54-7.52 (d, $J = 7.6$ Hz, 4H, 4Ar-H), 7.50-7.49 (d, $J = 4$ Hz, 2H, 2Ar-H), 7.04-7.02 (d, $J = 8.8$ Hz, 4H, 4Ar-H), 4.19-4.11 (m, 6H, 2HO- CH_2 , 2HO-CH), 3.91-3.78 (m, 4H, 2O- CH_2), 2.07-2.05 (m, 8H, 4Ar- CH_2), 1.24-1.07 (m, 152H, 76 CH_2), 0.89-0.85 (t, 12H, 4 CH_3), 0.74 (m, 8H, 4 CH_2CH_3). ^{13}C NMR (100 MHz, CDCl_3) δ (ppm) 157.94, 152.65, 151.83, 151.70, 146.46, 140.83, 139.65, 139.47, 138.32, 134.86, 132.82, 128.69, 128.31, 125.78, 125.72, 125.27, 124.86, 123.90, 121.07, 120.15, 120.07, 120.00, 114.87, 70.44, 69.34, 63.68, 55.35, 40.46, 31.95, 30.04, 29.73, 29.69, 29.63, 29.61, 29.39, 29.28, 23.83, 22.72, 14.16; HRMS, MALDI-TOF-MS m/z : Found 2194.6217 $[\text{M}+\text{H}]^+$. Calculated For $\text{C}_{146}\text{H}_{220}\text{N}_2\text{O}_6\text{S}_3$: 2193.6134.

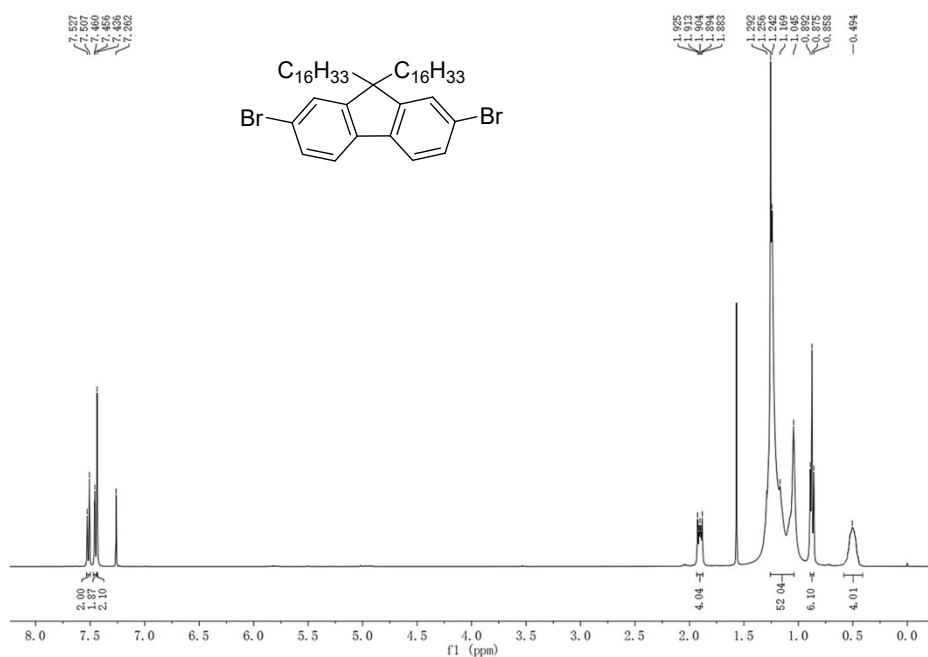


Fig. S8 ^1H NMR (CDCl_3 , 400 MHz ppm) spectra of representative compound **1/16** of **1/n**.

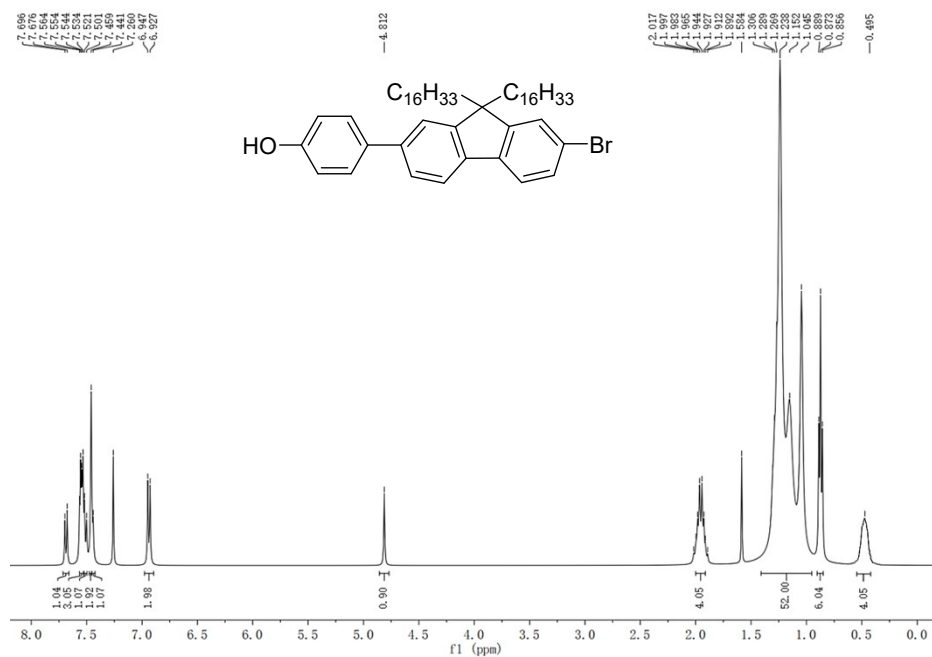


Fig. S9 $^1\text{H NMR}$ (CDCl₃, 400 MHz ppm) spectra of representative compound **2/16** of **2/n**.

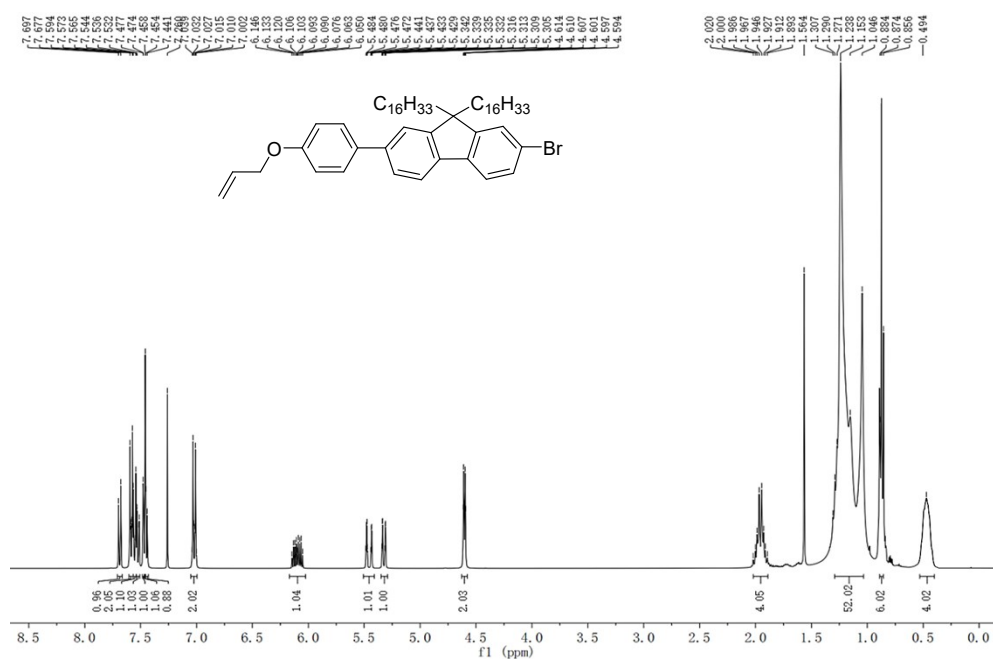


Fig. S10 $^1\text{H NMR}$ (CDCl₃, 400 MHz ppm) spectra of representative compound **3/16** of **3/n**.

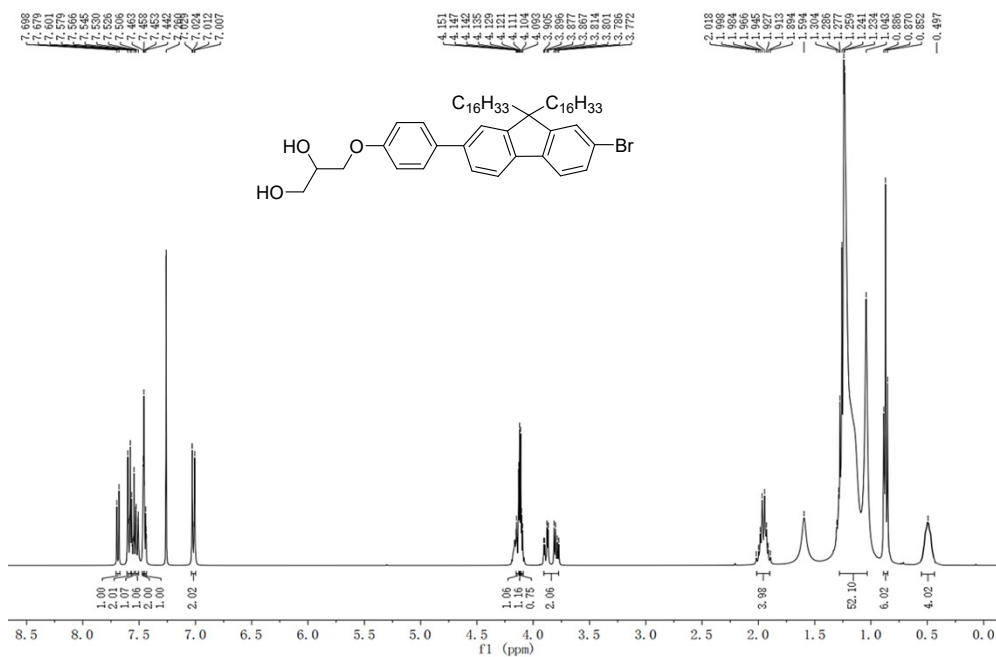


Fig. S11 ¹H NMR (CDCl₃, 400 MHz ppm) spectra of representative compound 4/16 of 4/n.

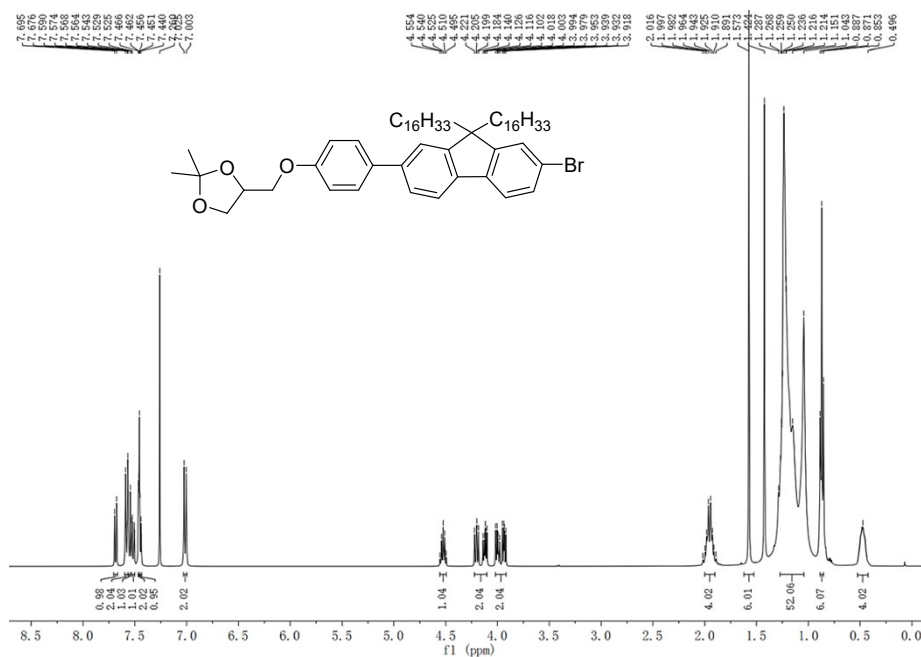


Fig. S12 ¹H NMR (CDCl₃, 400 MHz ppm) spectra of representative compound 5/16 of 5/n.

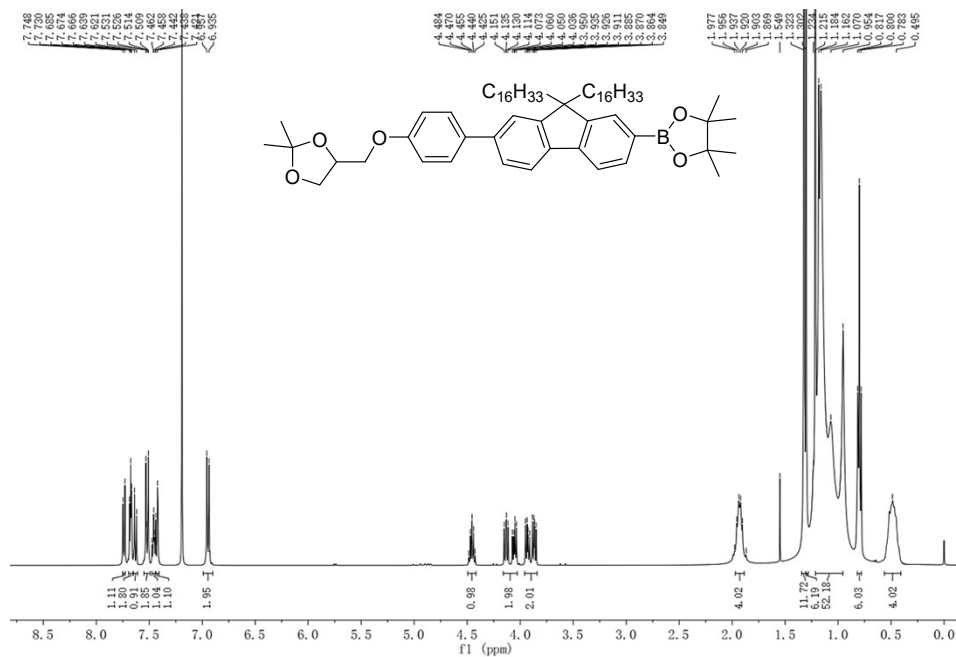


Fig. S13 ^1H NMR (CDCl_3 , 400 MHz ppm) spectra of representative compound **6/16** of **6/n**.

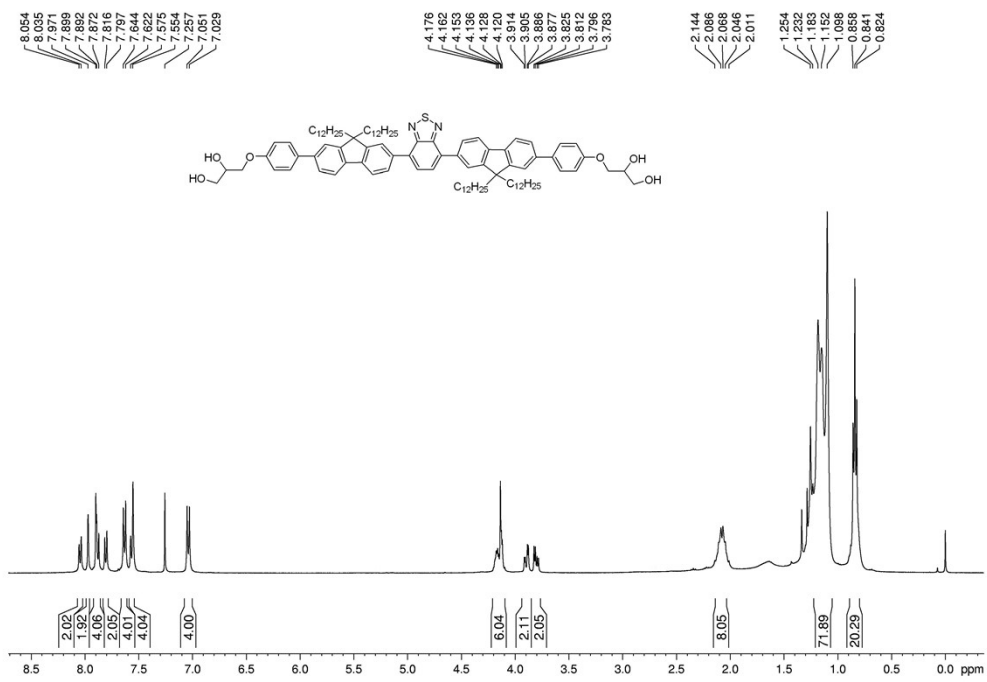


Fig. S14 ^1H NMR (CDCl_3 , 400 MHz ppm) spectra of **F12**.

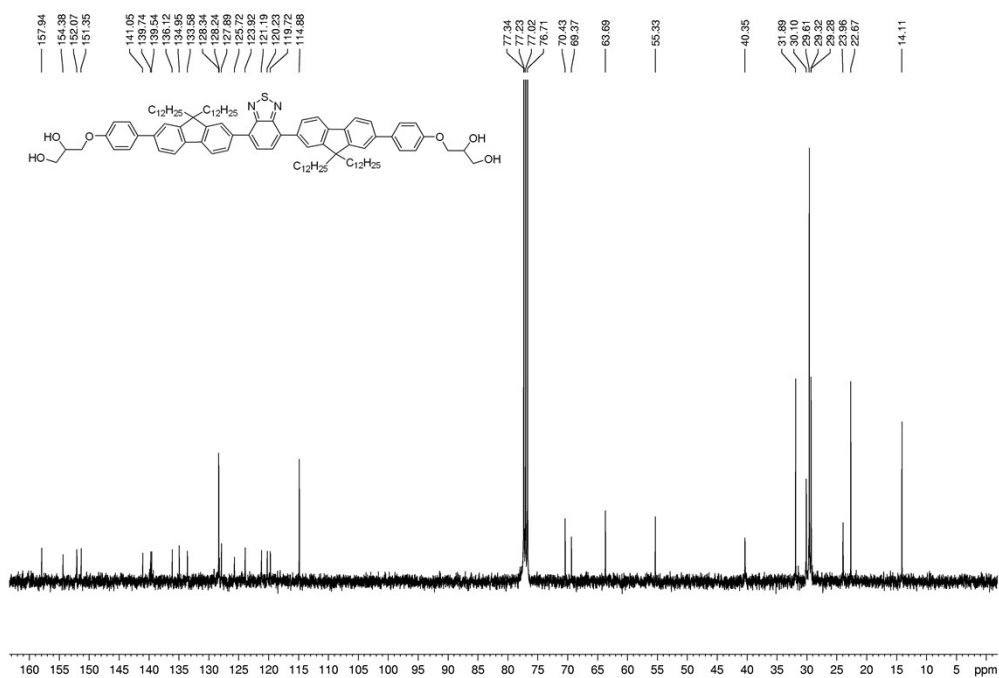


Fig. S15 ^{13}C NMR (CDCl_3 , 100 MHz ppm) spectra of **F12**.

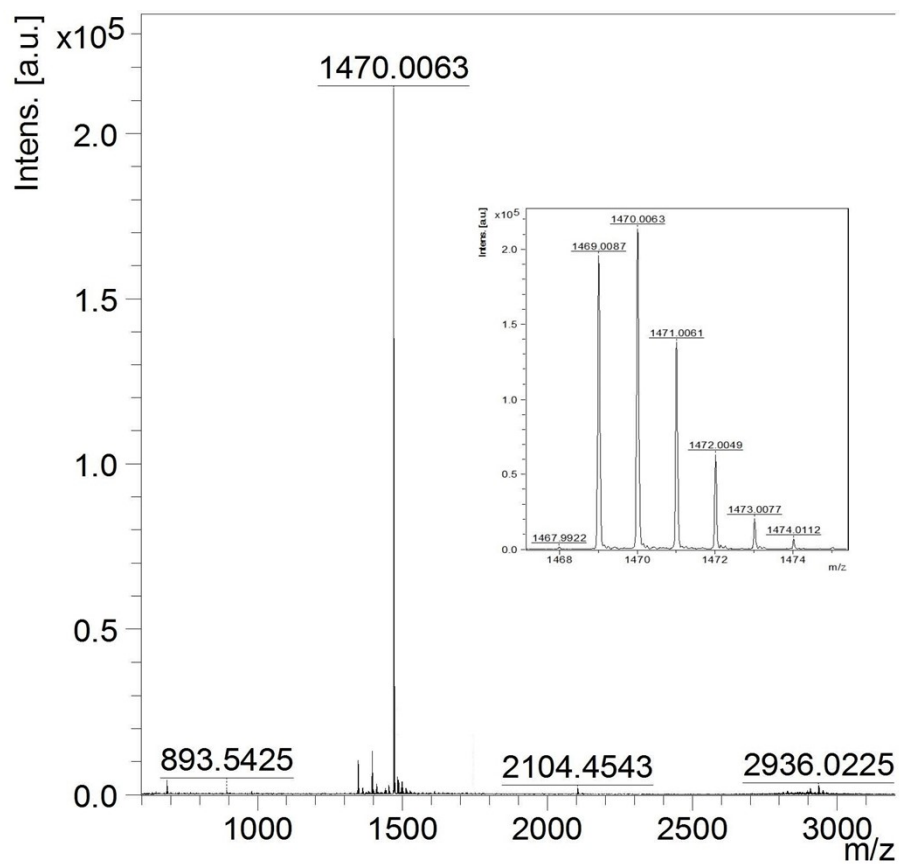


Fig. S16 HRMS spectrum of **F12**. MALDI-TOF-MS m/z : Found 1470.0063 $[\text{M}+\text{H}]^+$. Calculated For $\text{C}_{98}\text{H}_{136}\text{N}_2\text{O}_6\text{S}$: 1469.0119.

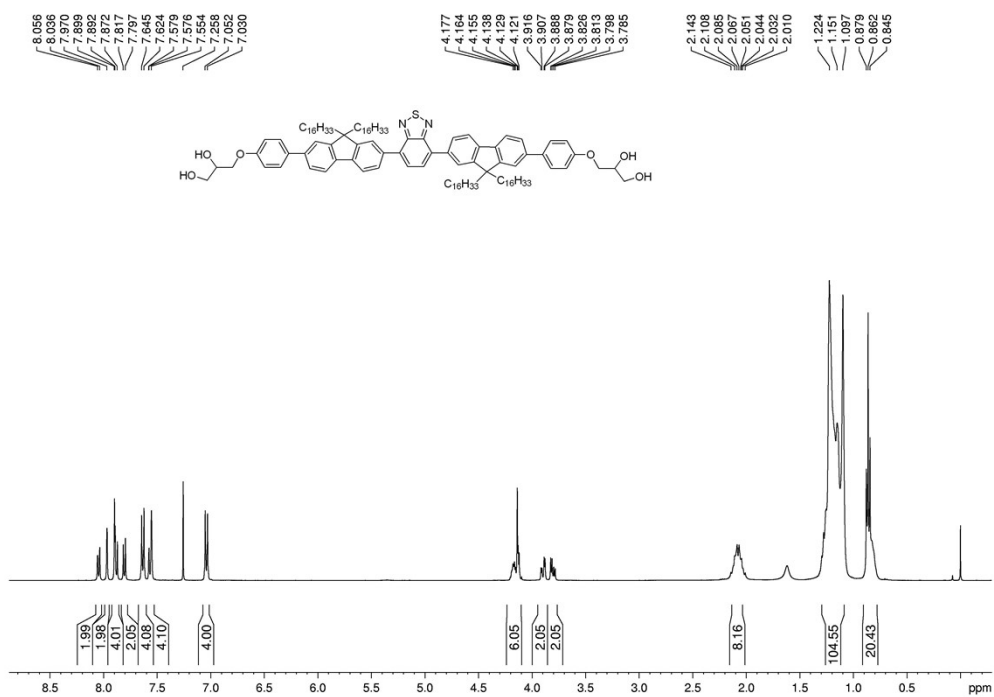


Fig. S17 ¹H NMR (CDCl₃, 400 MHz ppm) spectra of F16.

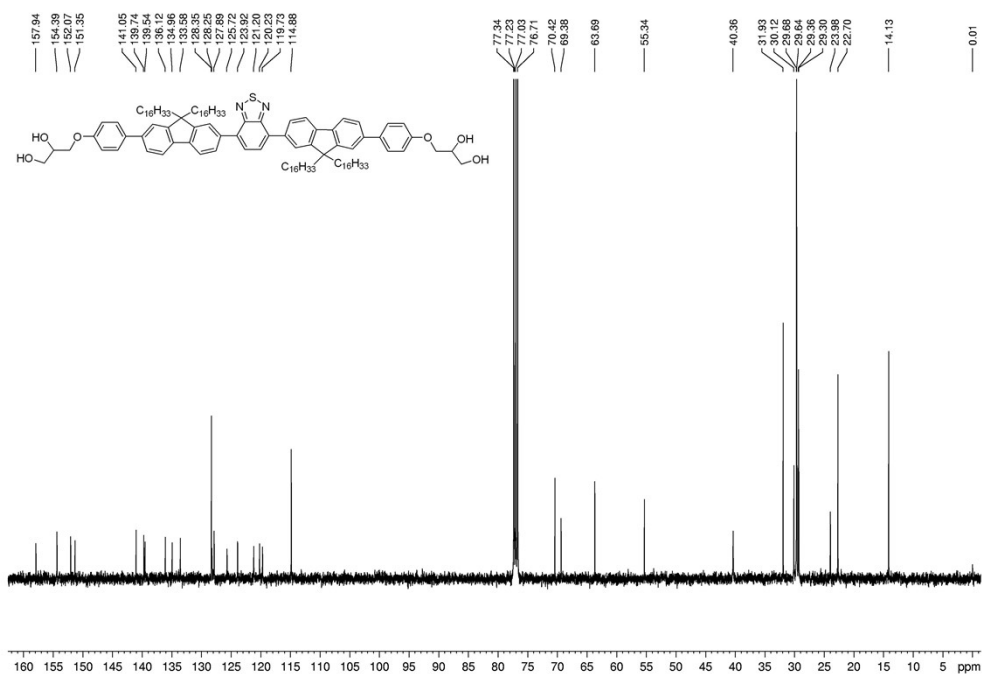


Fig. S18 ¹³C NMR (CDCl₃, 100 MHz ppm) spectra of F16.

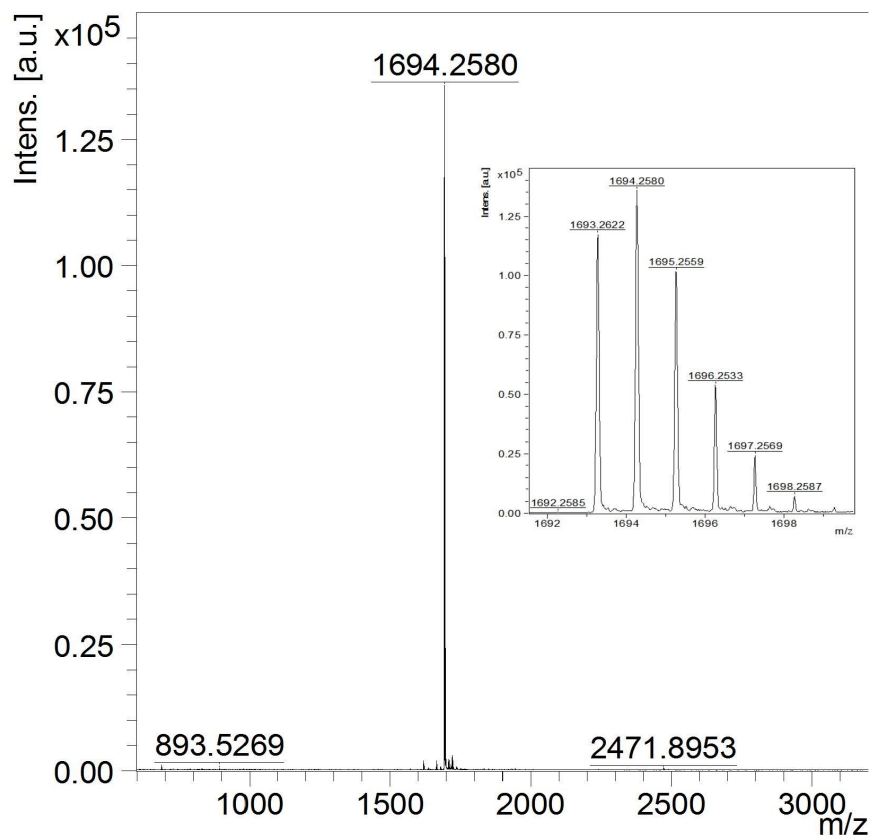


Fig. S19 HRMS spectrum of **F16**. MALDI-TOF-MS m/z: Found 1694.2580 [M+H]⁺. Calculated For C₁₁₄H₁₆₈N₂O₆S: 1693.2623.

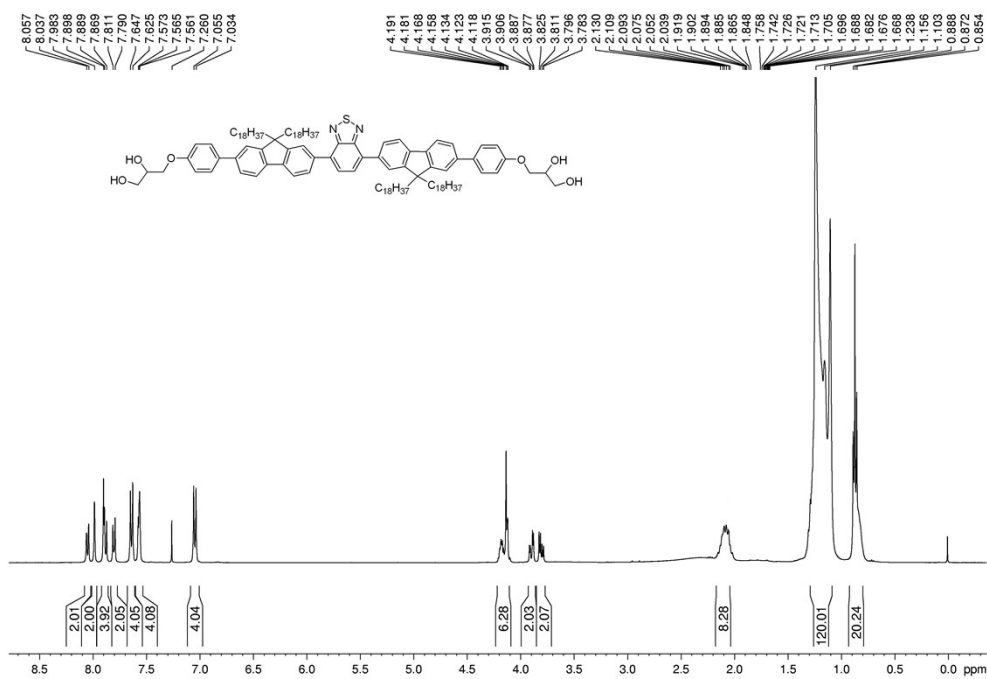


Fig. S20 ¹H NMR (CDCl₃, 400 MHz ppm) spectra of **F18**.

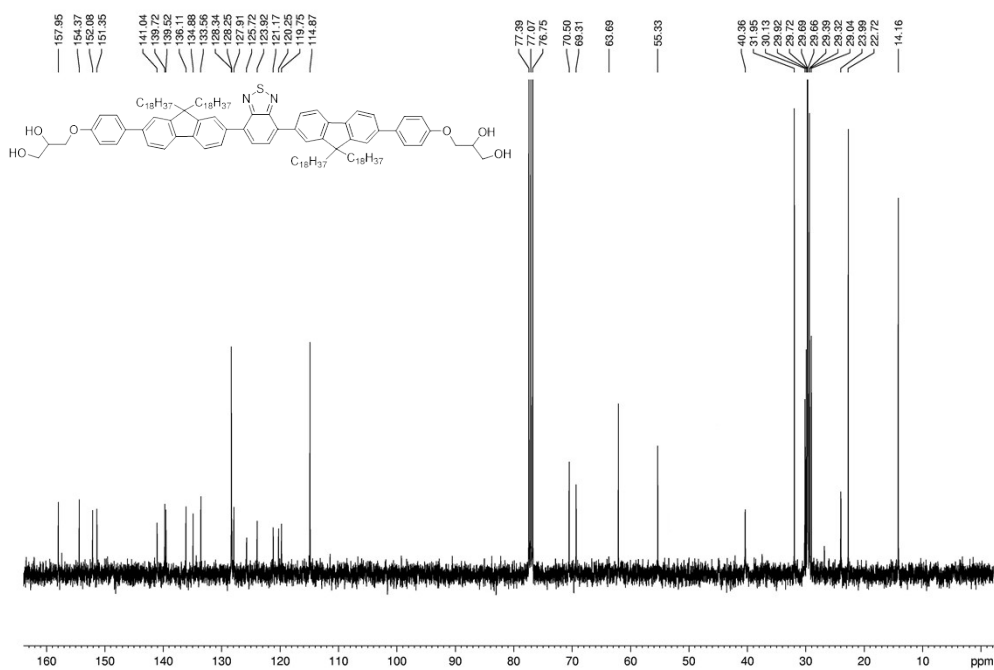


Fig. S21 ^{13}C NMR (CDCl_3 , 100 MHz ppm) spectra of **F18**.

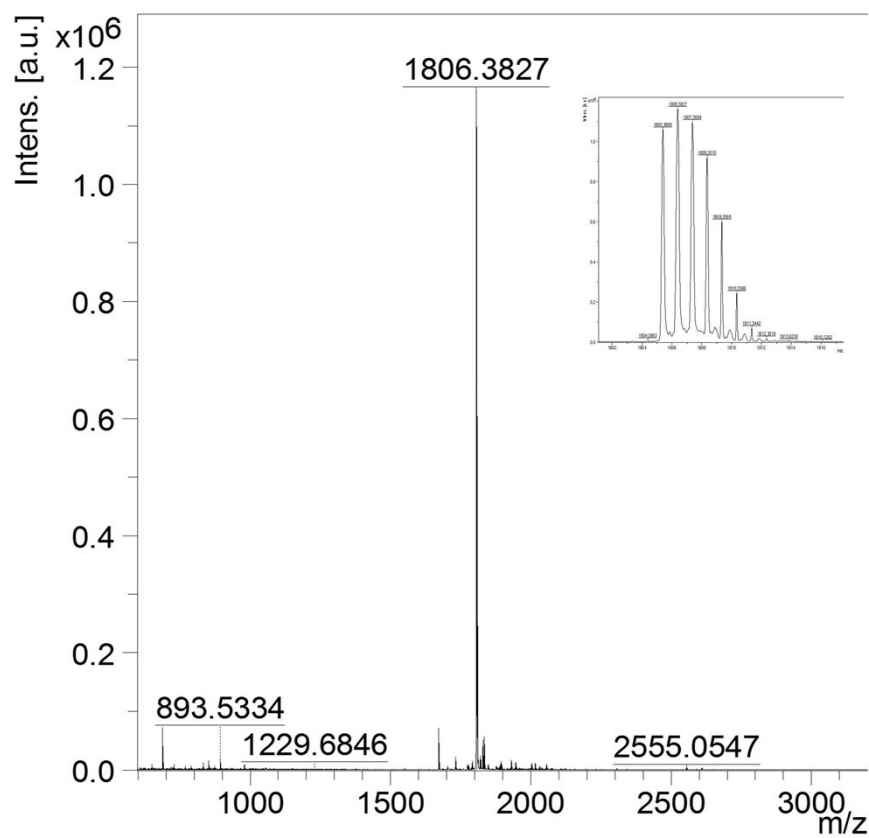


Fig. S22 HRMS spectrum of **F18**. MALDI-TOF-MS m/z : Found 1806.3827 $[\text{M}+\text{H}]^+$. Calculated For $\text{C}_{122}\text{H}_{184}\text{N}_2\text{O}_6\text{S}$: 1805.3875.

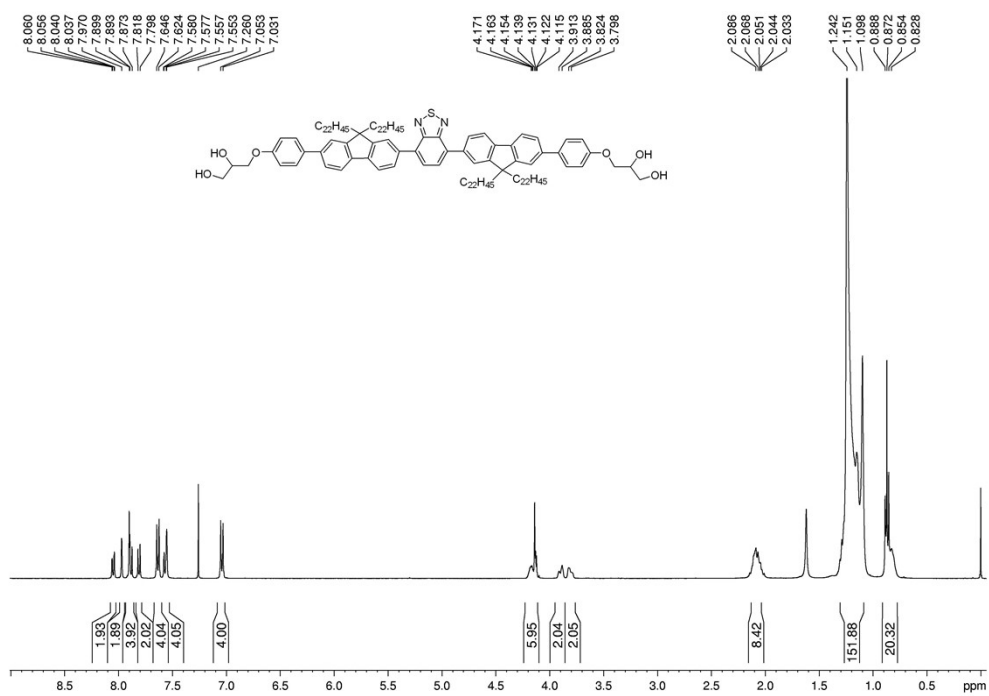


Fig. S23 ¹H NMR (CDCl₃, 400 MHz ppm) spectra of F22.

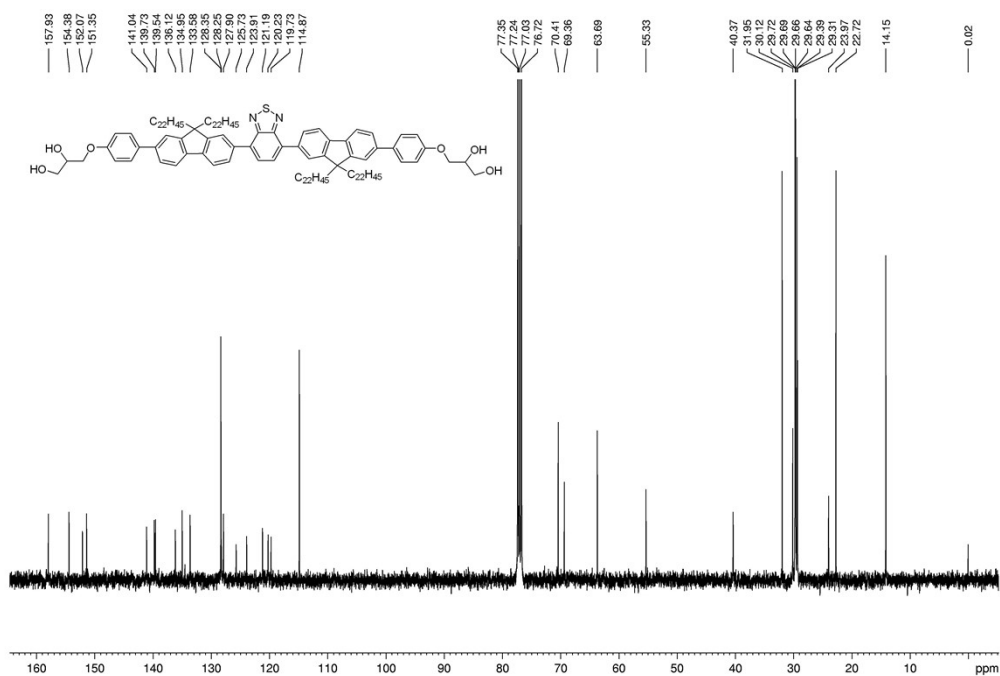


Fig. S24 ¹³C NMR (CDCl₃, 100 MHz ppm) spectra of F22.

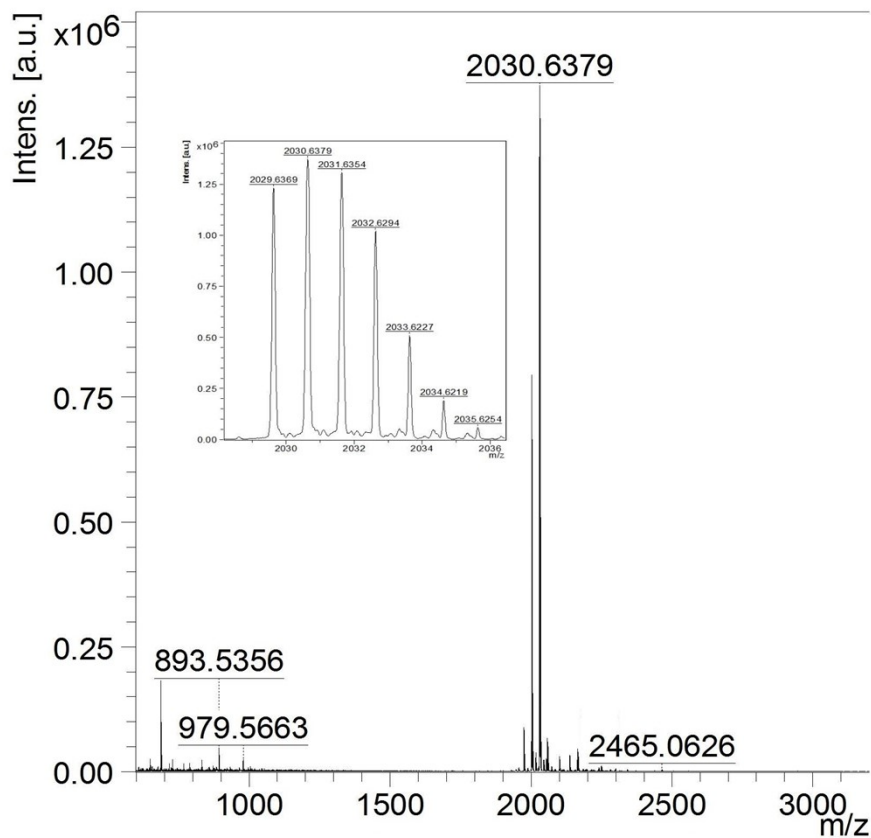


Fig. S25 HRMS spectrum of **F22** MALDI-TOF-MS m/z: Found 2030.6379 [M+H]⁺. Calculated For C₁₃₈H₂₁₆N₂O₆S: 2029.6379.

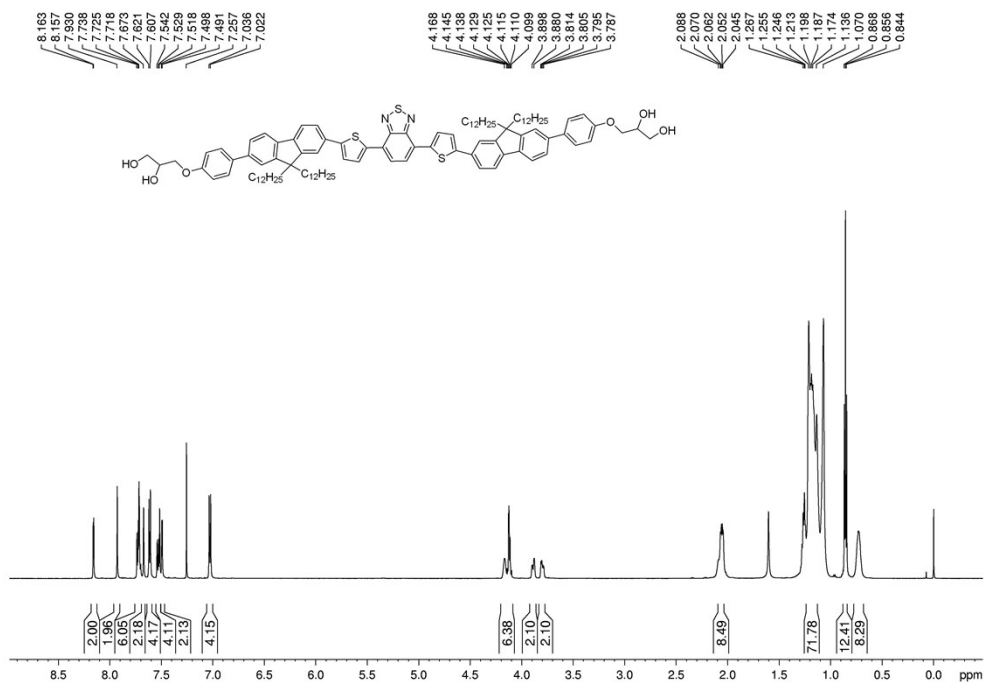


Fig. S26 ^1H NMR (CDCl_3 , 600 MHz ppm) spectra of **TF12**.

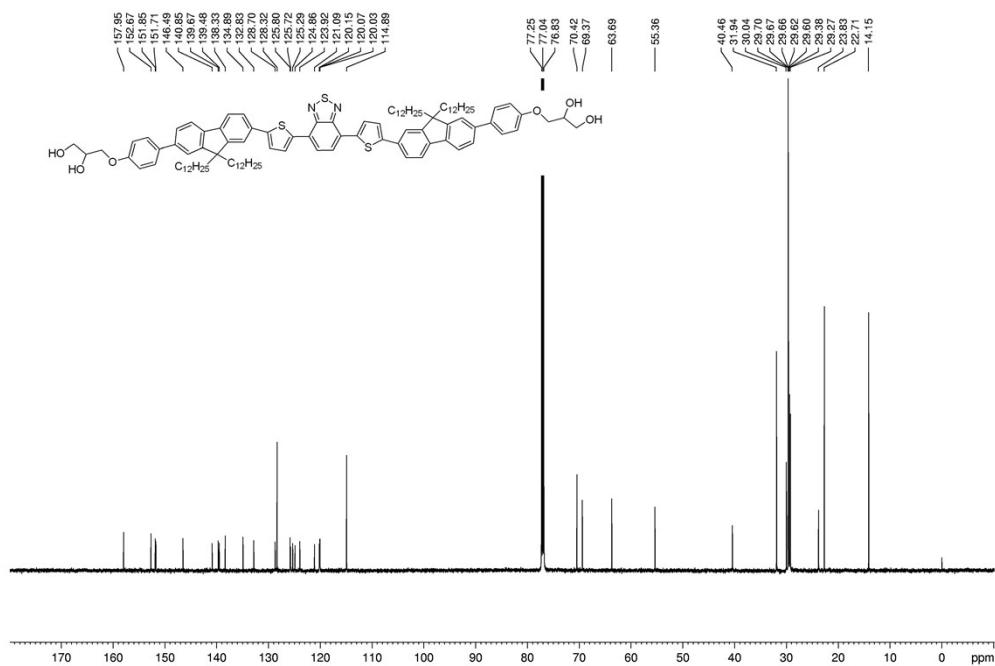


Fig. S27 ^{13}C NMR (CDCl_3 , 150 MHz ppm) spectra of **TF12**.

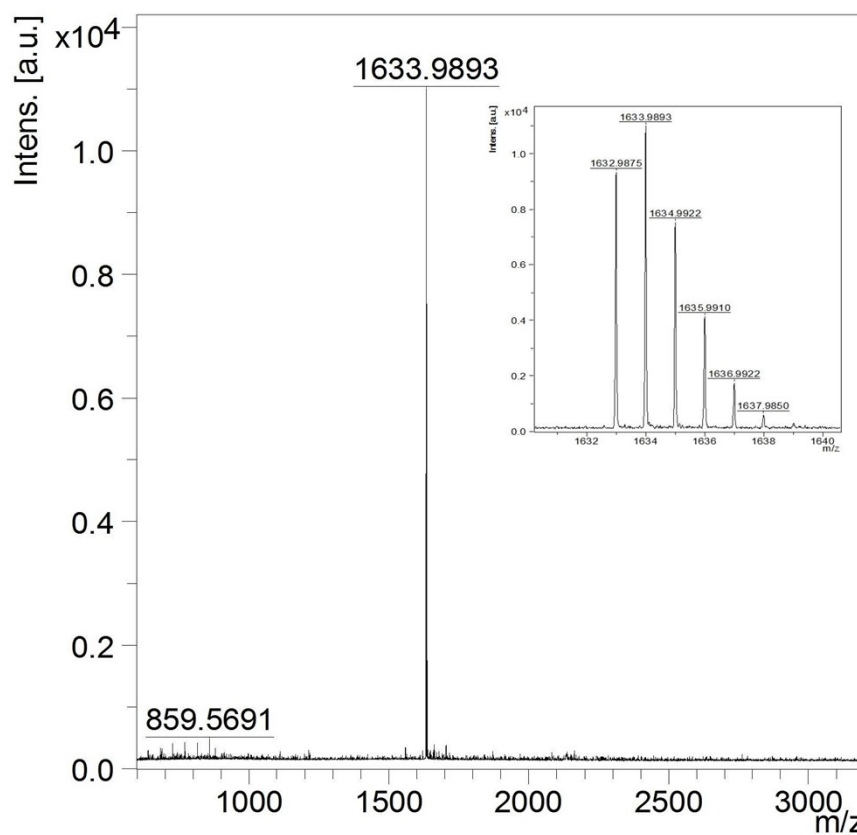


Fig. S28 HRMS spectrum of **TF12** MALDI-TOF-MS m/z : Found 1633.9893 $[\text{M}+\text{H}]^+$. Calculated For $\text{C}_{106}\text{H}_{140}\text{N}_2\text{O}_6\text{S}_3$: 1632.9874.

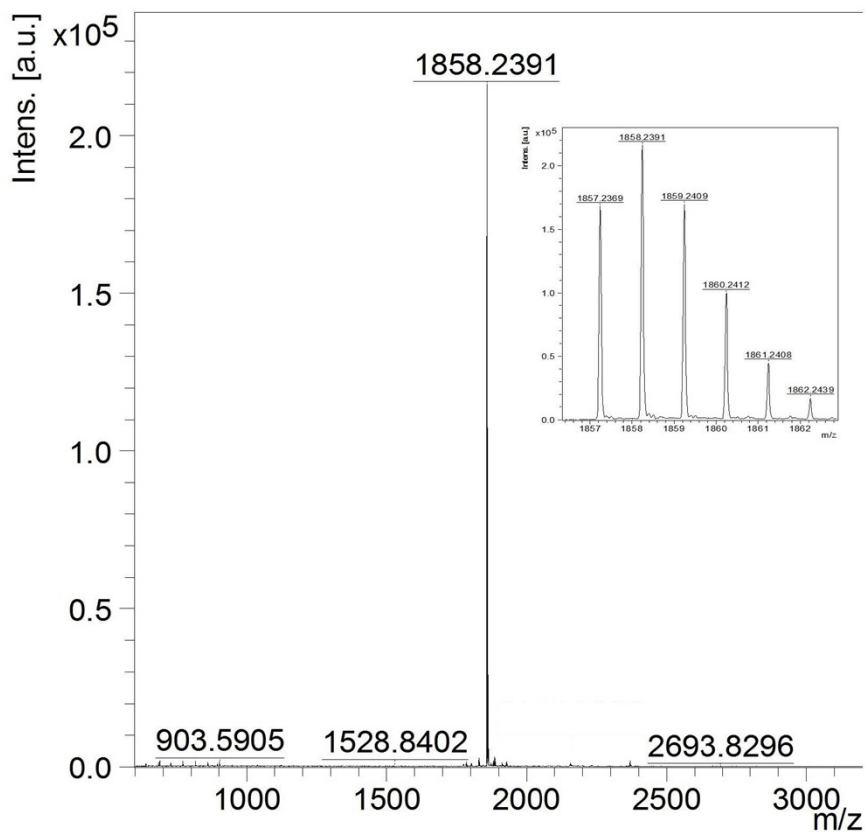


Fig. S31 HRMS spectrum of **TF16** MALDI-TOF-MS m/z: Found 1858.2391 [M+H]⁺. Calculated For C₁₂₂H₁₇₂N₂O₆S₃: 1857.2378.

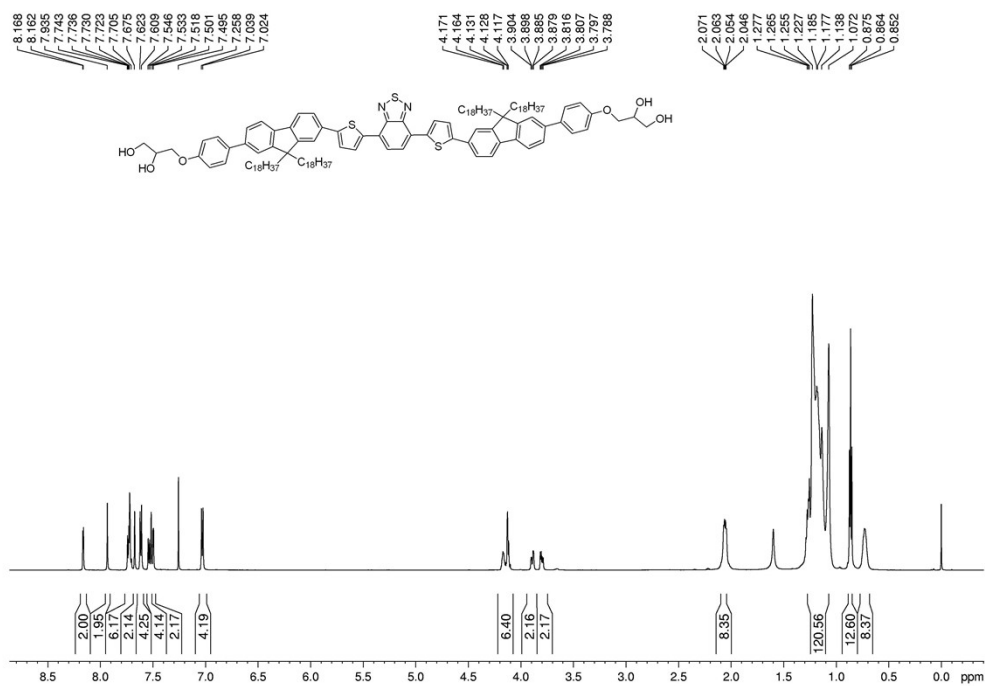


Fig. S32 ¹H NMR (CDCl₃, 600 MHz ppm) spectra of **TF18**.

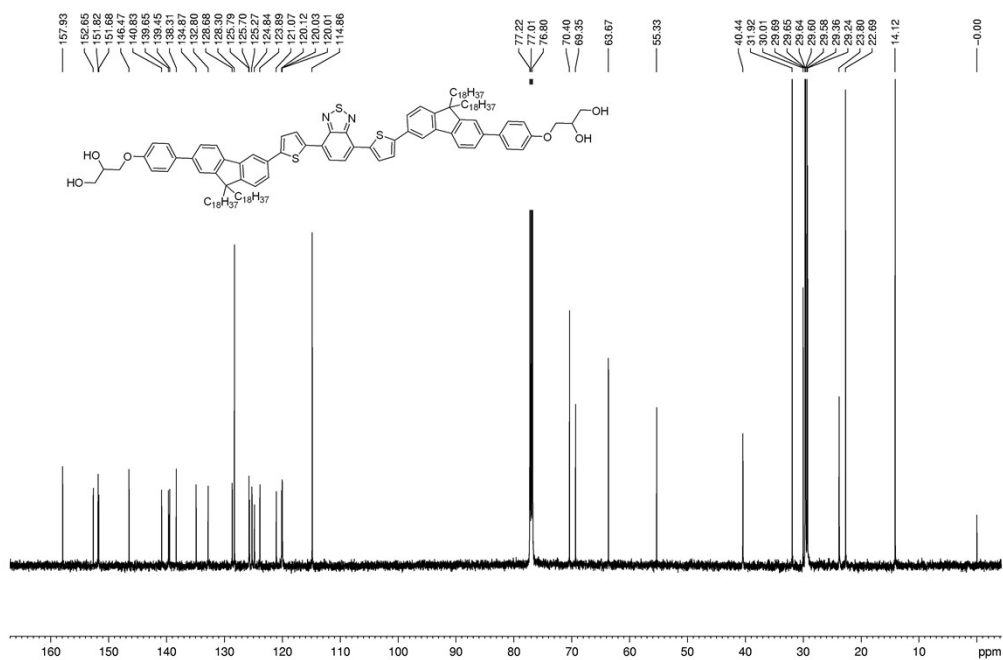


Fig. S33 ^{13}C NMR (CDCl_3 , 150 MHz ppm) spectra of TF18.

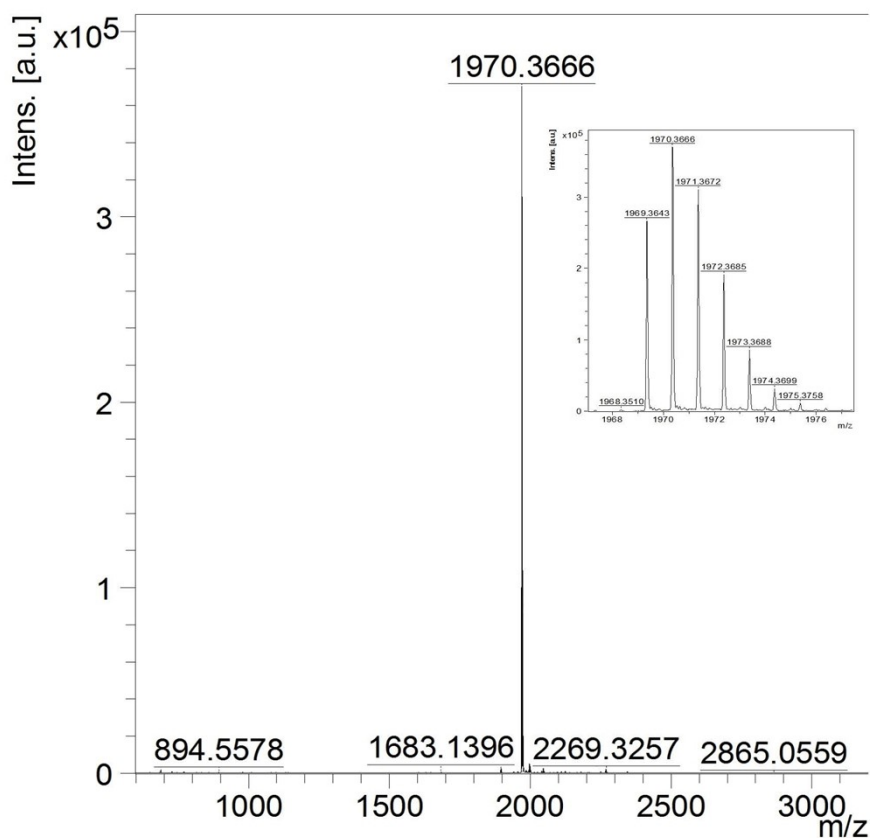


Fig. S34 HRMS spectrum of TF18 MALDI-TOF-MS m/z : Found 1970.3666 $[\text{M}+\text{H}]^+$. Calculated For $\text{C}_{130}\text{H}_{188}\text{N}_2\text{O}_6\text{S}_3$: 1969.3630.

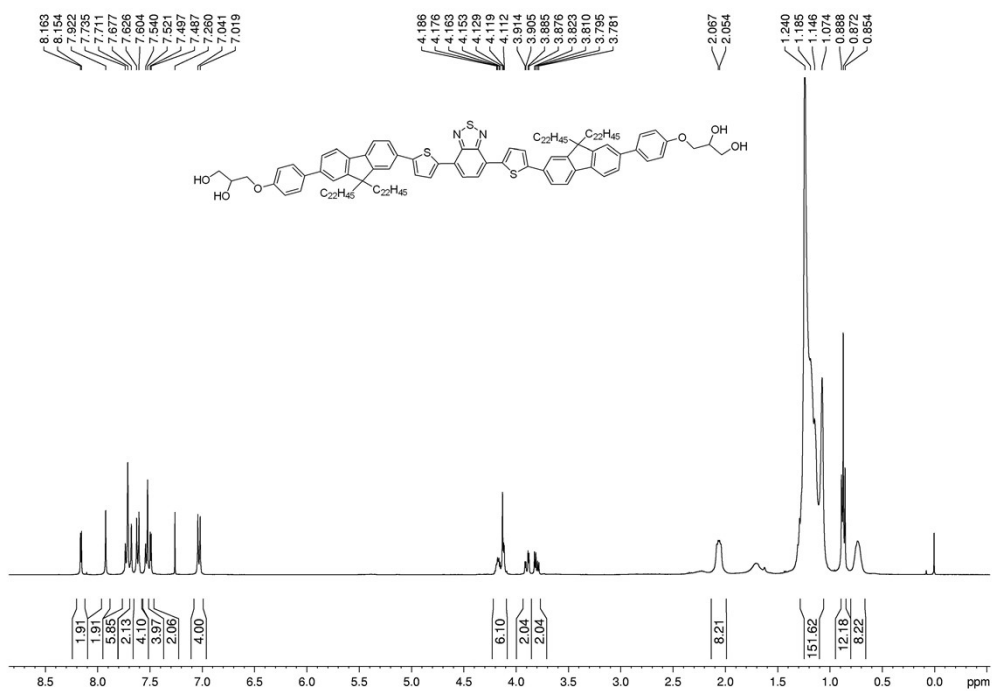


Fig. S35 ¹H NMR (CDCl₃, 400 MHz ppm) spectra of **TF22**.

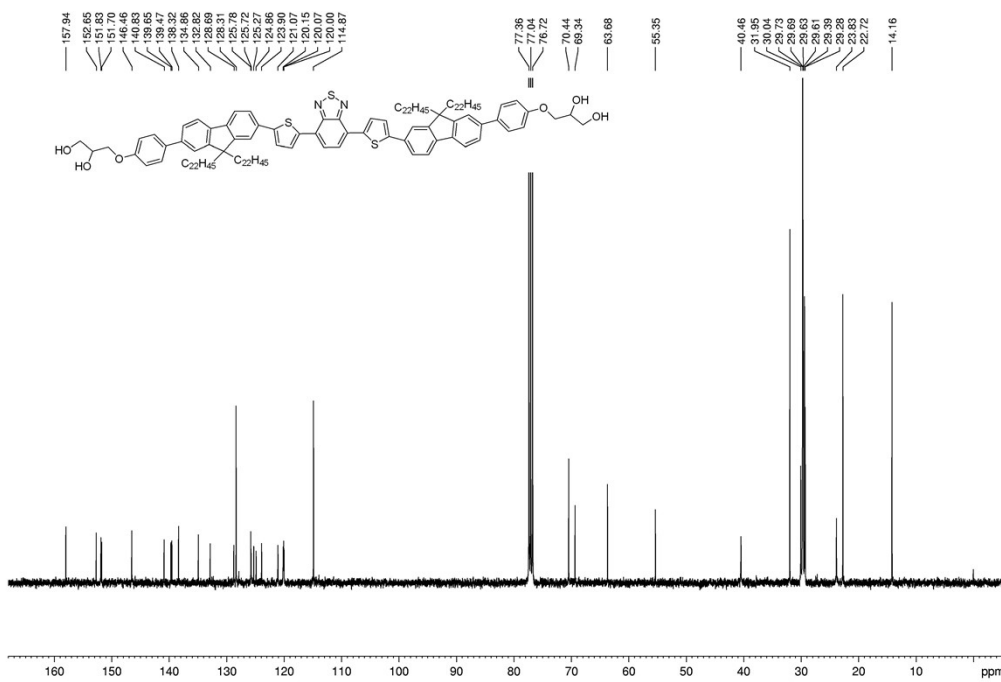


Fig. S36 ¹³C NMR (CDCl₃, 100 MHz ppm) spectra of **TF22**.

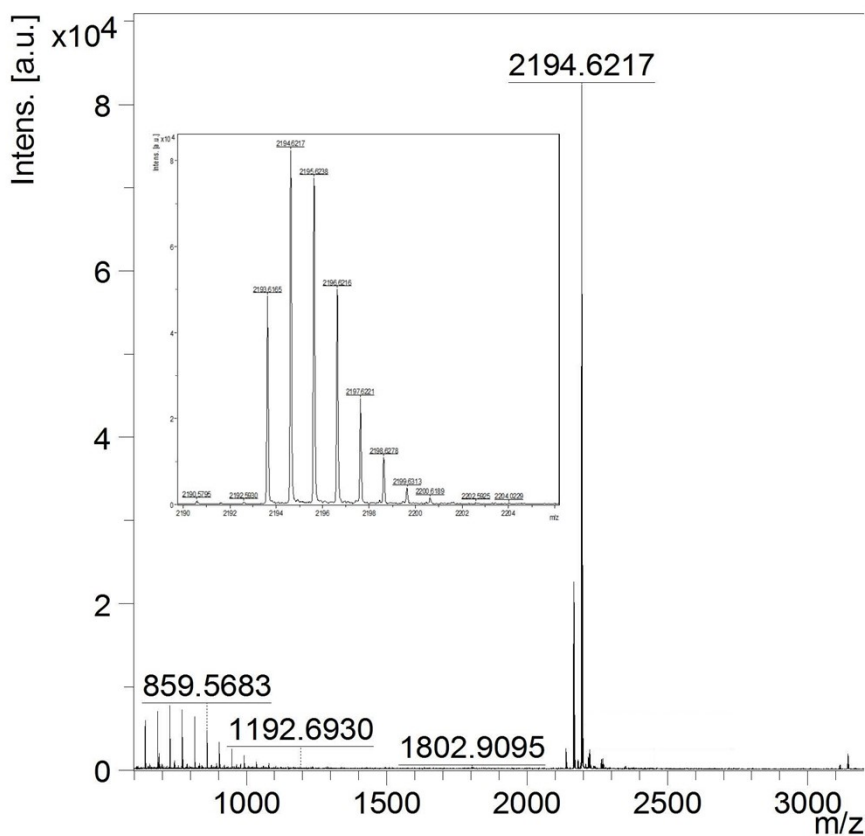


Fig. S37 HRMS spectrum of **TF22** MALDI-TOF-MS m/z: Found 2194.6217 [M+H]⁺. Calculated For C₁₄₆H₂₂₀N₂O₆S₃: 2193.6134.

3. References

- [S1] (a) C. A. Parker and W.T. Rees, *Analyst*, 1960, **85**, 587-600; (b) A.T. R. Williams, S. A. Winfield and J. N. Miller, *Analyst*, 1983, **108**, 1067-1071.
- [S2] *W. S. Sheldrick, Acta Cryst. B*, 1980, **36**, 2194.
- [S3] H. L. Liu, B. Qu, J. Chen, Z.Y. Cong, Z. W. An, C. Gao, L. X. Xiao, Z.J. Chen and Q. H. Gong, *J. Appl. Polym. Sci.*, 2013, **128**, 3250-3255.